Quantum Chemical Modeling of the Reduction of Quinones

J. R. Tobias Johnsson Wass,*,†,§ Elisabet Ahlberg,† Itai Panas,‡ and David J. Schiffrin§

Department of Chemistry, Electrochemistry, Göteborg University, S-412 96 Göteborg, Sweden, Department of Chemistry and Biotechnology, Chalmers University of Technology, S-412 96 Göteborg, Sweden, and Centre for Nanoscale Science, Department of Chemistry, University of Liverpool, Liverpool L69 7ZD, U.K.

Received: September 23, 2005; In Final Form: November 14, 2005

A systematic study of the redox properties of six parent quinones has been carried out using quantum chemistry methods. The reduction of the ortho (*o*-) and para (*p*-) isomers of benzoquinone and naphthoquinone, 9,10-anthraquinone and 9,10-phenantrenequinone to the corresponding hydroquinones and semiquinone radicals was investigated at the B3LYP/6-311+G(d,p) level of theory. Thermodynamic functions in the gas-phase were calculated for all the reduction reactions. Gibbs energies of reaction and standard potentials in water for the reductions were determined using the IEF−PCM model and an empirical correction to the calculations based on the limited thermodynamic data available for the quinones. Potentials were calculated both for the direct reduction to the quinols, and for the two-step reduction via the neutral semiquinones. The calculated potentials for the $2e^-$, $2H^+$ reductions were found in good agreement with experiment and to display the same trends as gas-phase enthalpies and energies, i.e., to correlate with the number of C═C double bonds, as well as on the relative position of the C═O groups. The small deviations between experiment and theoretically predicted standard potentials were found to originate from basis set incompleteness and the shortcomings in the B3LYP exchange correlation functional rather than the models used for the thermochemical calculations or description of solvation. Accurate theoretical shifts in standard potentials for the *p*-/*o*- pairs of Q ↔ HQ and HQ ↔ H_2Q reactions are presented and compared to experiment. Reliable standard potentials and shifts for the neutral semiquinones are predicted for the first time.

1. Introduction

1.1. Importance of Quinone Chemistry. Quinones are involved in the redox chemistry of virtually all living organisms and fulfill important biological functions. For example, ubiquinone-10, a 1,4-benzoquinone derivative, acts both as an electron carrier between the different components of the electron transport chain in the mitochondrion and as a redox component for the coupling of electron and proton transfer for the generation of pH gradients across the mitochondrial membrane (the Q cycle).[1,2] Compounds derived from naphtho- and anthraquinones also appear in important biochemical pathways. Naphthoquinone is the parent compound of vitamin K,[1] while anthraquinone is a basic component of many biological molecules.[3] Two natural naphthoquinones, alkannin and shikonin, are known to display wound healing, antiinflammatory, antibacterial, antirhombotic, topoisomerase inhibitory, and antitumor properties.[4] The best understood function of biological quinones is their involvement in electron-transfer reactions. The environment plays an important role in these reactions, for example, in controlling the bifurcation of the electron transfer from the $2e^-$ oxidant ubihydroquinone into two separate $1e^-$ transfers. In this case, quinone functionality is determined by the stability of the semiquinone radical, which in turn depends on the reaction environment.[5]

Another important area of quinone chemistry is in the industrial synthesis of hydrogen peroxide.[6] The detailed mechanism of these reactions is unclear, but electrochemical techniques can be used to map the course of quinone reduction and the reactivity of the intermediates with O_2. The electrochemical reduction of O_2 can proceed by a 4-electron mechanism to yield water or by a 2-electron mechanism to yield hydrogen peroxide. There is a considerable interest to find electrocatalysts that stop the reaction at the hydrogen peroxide stage since this would allow the simultaneous production of H_2O_2 and electrical energy in a fuel cell. Recent work has demonstrated that quinones can function precisely in this way[7−11] and that in this case, the reaction occurs between an electrochemically generated semiquinone and oxygen:

$$Q_{(\sigma)} + e^- \rightarrow Q_{(\sigma)}^{\bullet -} \qquad \text{(I)}$$

$$Q_{(\sigma)}^{\bullet -} + O_2(aq) \rightarrow Q_{(\sigma)} + O_2^{\bullet -}(aq) \xrightarrow{H_2O} H_2O_2 \qquad \text{(II)}$$

The quinone molecule $Q_{(\sigma)}$ in reactions I and II is chemically attached to a carbon electrode surface. The details of reaction II are still unknown. An important issue is the value of the redox potential of the $Q/Q^{\bullet -}$ couple, which strongly influences the kinetics of reaction. This potential depends strongly on the substituents present. The aim of the present work was to obtain basic thermodynamic data of quinones using quantum chemical calculations in order to provide a framework for the understanding of quinone-redox processes in aqueous media. As described above, quinone reactions of biological and industrial importance occur in water and the use of electrochemical information from nonaqueous solvents is of limited usefulness in particular, in relation to reaction mechanisms involving protonation reactions of intermediates. A detailed quantum chemical investigation of

† Göteborg University.
‡ Chalmers University of Technology.
§ University of Liverpool
* Corresponding author. E-mail: picard@chem.gu.se. Fax: +46 31 772 2853.

10.1021/jp055414z CCC: $33.50
Published on Web 01/14/2006

the reactions between quinones and O_2 will be presented in a subsequent publication.

The paper is divided into three sections. First, a brief description of the results from previous quantum chemical calculations for the quinones investigated and on the corresponding redox potentials is presented, as well as a summary of the available experimental standard potentials data. Second, quantum chemical calculations are carried out for the various molecules involved in the redox chemistry of the *p*- and *o*-isomers of benzo- and naphthoquinone, and for 9,10-anthraquinone and 9,10-phenanthrenequinone. The results of the calculations comprise thermodynamic functions for the reduction reactions in the gas-phase, as well as Gibbs energies of reduction and standard potentials in water. Finally, the results of these calculations are compared with experimental data.

2. Background and Methods

2.1. Previous Quantum Chemical Calculations. Quantum chemical calculations have been previously carried out to investigate quinone compounds as models for ubiquinone, plastoquinone (another BQ derivative) and for the two natural forms of vitamin K (phyllo- and menaquinones).[12−17] These studies provided accurate vibrational spectra, hyperfine coupling constants and **g**-tensors for the quinones and their radical anions. The calculation of redox potentials of quinones in aqueous solutions has attracted considerable attention. Reynolds[18−20] used the two wave function based methods Hartree−Fock (HF) and Møller−Plesset second-order perturbation theory (MP2) for calculations on benzo- and naphthoquinones. Wheeler[21] applied HF, MP2, and density functional theory (DFT) using the B3LYP functional for calculation on benzoquinone. The work of the Wheeler group was subsequently extended to chloro-substituted BQs using B3LYP only.[22] Rzepa et al.[23] and Namazian et al.[24−30] investigated the standard potentials for various quinones using semiempirical methods (MNDO, PM3, AM1),[23−25] as well as the HF[24,26] and B3LYP methods.[26,27] Namazian et al. have also extended their investigations to calculations of potentials in nonaqueous solvents.[28−30] Recent studies on disulfonated anthraquinone by Rosso et al.[31] employing B3LYP calculations have shown good correlation with experimental results.

Two different methodological approaches were applied in these studies, both employing thermodynamic cycles. That of Reynolds,[18−20] Rzepa et al.[23] and Namazian et al.[24−30] used isodesmic reactions (e.g., $Q'H_2 + Q \rightarrow QH_2 + Q'$) in order to calculate Gibbs energies of reaction relative to a reference system ($Q'/Q'H_2$). Both 1,4-BQ and 1,4-NQ were used for this purpose but the results were somewhat dependent on the reference quinone used. Since different reference systems predicted different potentials, it is difficult to verify the validity of a specific reference without comparing each calculated potential to experimental values, which limits the predictive power of this method. A second approach was taken by Wheeler et al.,[21,22] Namazian et al.[27] and Rosso et al.,[31] in which electrons and protons were used explicitly as the reference system for the reactions. This is a direct approach since it requires calculations to be carried out for one quinone only in order to obtain a specific potential.

Two strategies for calculating the approximate Gibbs energies of solvation were used in the previous works. Reynolds and Wheeler used a free energy perturbation (FEP) method in conjunction with molecular dynamics[18−22] whereas Rzepa and Namazian used the polarized continuum models (PCM), which are less computationally demanding. The calculated reduction potentials using these techniques were generally within 10−100 mV of the experimental values.

Although the results from these investigations were in approximate agreement with experimental data, several of the calculations were performed with small basis sets, e.g. missing polarization functions on the H atoms or lacking diffuse functions. Only few studies have employed basis sets that are reasonably large and balanced in their description of all atoms in the molecule. Eriksson et al. studied structural, electronic and magnetic properties of species in the 1,4-BQ system using B3LYP and the 6-311G(d,p) basis set.[32] However, the larger 6-311+G(2df,p) basis set was used for calculating, e.g., electron affinities. Basis set effects were observed for this specific property, but no systematic investigation of trends were made. Investigations of the electron affinity of 1,4-BQ using DFT methods as well as high-level wave function based methods have recently been carried out by Kim et al.[33] The basis set convergence was, however, not investigated, although large basis sets are necessary when using these methods in order to achieve an accurate description of electron correlation.

2.2. Experimental Measurements of Standard Potentials. The redox properties of quinones have been investigated for a long time. The accuracy of standard potentials measurements varies, and, e.g., for 9,10-anthraquinone, the low solubility of the quinone in water makes an exact determination of its standard potential difficult. For the less soluble components of the quinone series, information is available for voltammetric measurements carried out for the quinone adsorbed on carbon electrodes. There is a problem with these data when assessing the interactions with the surface and to what extent these affect the value of the measured redox potentials.

The most important literature data[34−51] on the standard potential of the quinones investigated are presented in Table 1, and in what follows, the reasons for the choice of the particular values employed in the comparison with the quantum chemical calculations are discussed. The data presented in Table 1 have been corrected to pH = 0 when necessary. The values reported are formal potentials ($E^{\circ\prime}$) since activity coefficient corrections have not been performed.

2.2.1. *o*-Benzoquinone (1,2-BQ). The long-term stability of the aqueous solutions of this quinone is very poor, with clear evidence of decomposition. The results by Conant and Fieser[34] are therefore unreliable since the potentiometric measurements (titration curve method) were carried out in solutions were condensation reactions were taking place. In contrast, the measurements by Proudfoot and Ritchie[35] were obtained by the in situ oxidation of benzene-1,2-diol in a cyclic voltammetric experiment. In this case, the time scale of the experiment was very short and interference by oxidation reaction of the quinone formed did not affect the measured potentials. For this reason, the value reported in these experiments of 0.831 ± 0.016 V was employed as the most accurate experimental value of the standard potential.

2.2.2. *p*-Benzoquinone (1,4-BQ). Hale and Parsons[36] studied the electrochemistry of mixtures of the quinones and the corresponding quinols using a dropping mercury electrode. The solutions were very sensitive to adventitious leakage of oxygen from the air. A quasi-reversible behavior was observed which might account for the discrepancy in the values obtained with those reported form equilibrium measurements (see below). Similar considerations apply to the results by Driebergen at al.[38] who employed the same electrode. The half-wave potential was measured as a function of pH but no corrections for the irreversibility of the reaction were taken into account. The work of Bailey and Ritchie[39] employed cyclic voltammetry to measure the half-wave potential of 1,4-BQ and several aqueous solutions

TABLE 1: Summary of Literature Data for the Values of the Standard Potentials of the Quinone/Quinol Couples in Aqueous Solutions

1,2-BQ	potential vs NHE/V	ref	comments
i	0.787 ± 0.001	34	obtained by potentiometric titration of quinone solutions with Ti^{3+}, where the value of $E^{\circ\prime}$ for the 0.1 M HCl solution was chosen to minimize possible errors due to the protonation of the quinone
ii	0.831 ± 0.016	35	cyclic voltammetry of solutions of benzene-1,2 diol (catechol) on a gold electrode at different pH values

1,4-BQ	potential vs NHE/V	ref	comments
iii	0.659	36	dropping Hg electrode. From BQ + BQH_2 solutions at pH 3.9, with measurement at only one pH.
iv	0.709	37	adsorbed on highly ordered pyrolytic graphite (HOPG) from 0.2 to 2 μM solutions, with results calculated from cyclic voltammetry
v	0.636[a]	38	dropping Hg electrode, where only the quinone was present in the solution and the halfwave potentials were determined at 20 °C
vi	0.694	39	cyclic voltammetry on a Au electrode, where only the quinone was present in solution.
vii	0.6990 ± 0.001	40	quinone in solution. No quinhydrone formation could take place. The measurement was made by potentiometric titration with Ti^{3+}

1,2-NQ	potential vs NHE/V	ref	comments
viii	0.566	41	ac voltammetry on glassy carbon, where the solutions under study contained the dissolved quinone in M $HClO_4$ and the measurement corresponds to the adsorbed quinone
ix	0.565	42	DPV results (no NQ concentration reported) pH = 2.0; the value reported here has been corrected to pH = 0
x	0.547 ± 0.002	34,43	the results were obtained by measuring the potentials at different stages of titration of a 1,2-NQ solution with Ti^{3+}

1,4-NQ	potential vs NHE/V	ref	comments
xi	0.514	36	same as entry iii but using a NQ + NQH_2 solutions (Hg); pH = 3.9, where the results were corrected for pH
xii	0.446	41	same as entry vii; ac voltammetry on glassy carbon, where the solutions under study contained the dissolved quinone. The measurement corresponds to the adsorbed quinone and not to the species in solution
xiii	0.464	37	adsorbed on HOPG from 0.2 to 2 μM solution, with results calculated from cyclic voltammetry
xiv	0.424	44	Q+QH_2 mixed with carbon, where the equilibrium potential of this mixture was measured for different values of the pH.
xv	0.440	38	same as entry v, where a dropping Hg electrode was used, and only the quinone was present in the solution and the half wave potentials were determined at 20 °C
xvi	0.485	39	same as entry vi; cyclic voltammetry on a Au electrode, where only the quinone was present in solution.
xvii	0.470 ± 0.002	40,43	potentiometric measurement, for titration of NQ with Ti^{3+}; NQ only was present in the solution

9,10-AQ	potential vs NHE/V	ref	comments
xviii	0.106	41	ac voltammetry on glassy carbon, where the solutions under study contained the dissolved quinone; the measurement corresponds to the adsorbed quinone.
xix	0.124	37	adsorbed on HOPG from 0.2 to 2 μM solutions, with results calculated from cyclic voltammetry
xx	0.110	45	carbon surface chemically grafted with 1-AQ
xxi	0.079	45	carbon surface chemically grafted with 2-A−Q
xxii	0.124	46	AQ grafted at position 1; measurement in 0.5M H_2SO_4; corrected for pH.
(xxiii)	0.05	47	AQ grafted on a diamond electrode and measurements carried out in 0,1 M KOH, where the potential of the Q/Q^{-2} couple was measured and corrected for p*K*. $pK_1 = 9.7$; $pK_2 = 12.05$

9,10-PQ	potential vs NHE/V	ref	comments
xxiv	0.446	41	ac voltammetry on glassy carbon, where the solutions under study contained the dissolved quinone and the measurement corresponds to the adsorbed quinone
xxv	0.439	48	adsorbed onto pyrolytic graphite from a 10^{-6} M solution. Cyclic voltammetry.
xxvi	0.432	37	adsorbed on basal plane pyrolytic graphite from 0.2 to 2 μM solutions, with results calculated from cyclic voltammetry
xxvii	0.431	49	voltammetry of PQ absorbed on HOPG. data in $HClO_4$ corrected to pH = 0
xxviii	0.445	50	voltammetry of PQ adsorbed on a carbon paste electrode [$HClO_4$] = 0.1M; corrected for pH
xxix	0.442 ± 0.002	51	potentiometric titration with Ti^{3+}; quinone present in solution; no interference by possible formation of the quinhydrone

[a] T = 20 °C.

of sulfonate derivatives since these provided good solubility. This approach requires an analysis of the current−potential dependence to extract thermodynamic information from a nonequilibrium system. Their results were close to those obtained from very careful equilibrium measurements by LaMer and Baker,[40] using a potentiometric titration method. Similar results were also reported in ref 34. The value in ref 40 (entry vii in Table 1) was accepted as the most accurate determination of the standard potential for this quinone since LaMer and Baker calculated the standard potential from the whole potentiometric titration curve rather than taking the value at a particular point.

2.2.3. *o*-Naphthoquinone (1,2-NQ). The poor solubility of this compound and that of the other larger quinones presents serious difficulties for the measurement of their standard potentials. For this quinone, its properties when adsorbed on glassy carbon electrodes have been investigated (entries viii and ix) and these studies give similar values of $E^{\circ\prime}$. The values reported in refs 34 and 43 are more accurate since they refer to

full titration curves of species in solution. For this reason, the value given by Conant and Fieser in entry x[34] was employed as the standard potential for 1,2-NQ.

2.2.4. *p*-Naphthoquinone (1,4-NQ). Three different types of measurements have been carried out. The $E^{\circ\prime}$ value by Hale and Parsons[36] is too positive, and this may be related to the way the equilibrium potentials was calculated for nonequilibrium conditions that required a diffusion-activated reaction model for abstracting the standard potential from the current−potential curves. The same problem appears to apply to entry xv. Entries xii and xiii correspond to measurements of the adsorbed quinone. Entry xiv[44] is an equilibrium measurement. However, in this case, the equilibrium involves the *solid* quinone/quinol phases and hence, these results do not correspond to the properties of the solution species that were calculated in the present work by quantum chemistry methods. The most reliable measurements for this quinone are those of LaMer and Baker,[40] who employed a potentiometric titration of the quinone with Ti^{3+} and calculated average values of $E^{\circ\prime}$ at many points in the titration curve.

2.2.5. 9,10-Anthraquinone (9,10-AQ). No data could be found in the literature for the standard potential of this quinone in aqueous solutions. The reason for this is the very low solubility of this compound in water. The only data that can be used for the evaluation of the standard potential are those derived from voltammetric measurements for the adsorbed or chemically attached quinone on inert electrodes. Carbon has been used as a support in voltammetric studies of adsorbed 9,10-AQ. Schreuers at al.[41] measured the reduction of the quinone adsorbed from its saturated aqueous solution. The equilibrium potentials of mixture of anthraquinone, anthraquinol and carbon as a function of pH was measured by Binder at al.[44] From these results, the potential at pH = 0 was 0.118 V vs the NHE. Since this result corresponds to the solid phase (and to the quinhydrone), this value is not comparable with the calculations in this paper.

Entries xx−xxiii correspond to carbon surfaces that have been chemically functionalized with 9,10-AQ. This approach has the advantage that the quinone is not specifically adsorbed to the carbon but rather it is chemically bonded, for instance by the reduction of the corresponding diazonium salt. It would be expected that this approach would produce a more reliable value of $E^{\circ\prime}$ since this would be equivalent to measuring the properties of a substituted quinone. However, it is not possible to correct for the inductive effect of the surface on the redox potential. The measurements from alkaline solution are based on the indirect measurement of the surface concentration of quinone species as a function of potential based on the reactivity of the semiquinone radical with oxygen. Although the deconvolution of the oxygen reduction current in different contributions can be carried out successfully, there is a great deal of uncertainty in the p*K* values required to transform these measurements to pH = 0. Because of these uncertainties, only a range in the likely value of the $E^{\circ\prime}$ for this compound can be given and in the absence of better information, the average of all the above determinations was taken. The likely range of values for this quinone is $E^{\circ\prime} = (0.09 \pm 0.03)$ V.

2.2.6. 9,10-Phenanthrenequinone (9,10-PQ). Entries xxiv−xxviii correspond to cyclic voltammetry measurements for this quinone adsorbed on various carbon electrodes. The average of all these determinations of $E^{\circ\prime}$ is 0.439 ± 0.006 V. $E^{\circ\prime}$ has been measured from solution using a potentiometric titration technique.[51] This determination made use of all the points in the titration curve. The value of $E^{\circ\prime}$ calculated was 0.442 V, in reasonable agreement with the results obtained for adsorbed 9,10-PQ and was used to compare with calculations.

2.3. Computational Techniques.

2.3.1. General Considerations. The hybrid Hartree−Fock (HF)/density functional theory (DFT) method B3LYP[52] was used for the calculations. B3LYP was selected as the preferred method since extensive investigations have demonstrated that it can be applied successfully to different types of chemical systems.[53] Close agreement with experimental results and with explicitly correlated wave function based quantum chemical methods were obtained in these studies. In the present work, the quality of some of the B3LYP results was tested by comparisons with several such methods, including Møller−Plesset perturbation theory of second and higher orders (MP2, MP3, and MP4) and coupled cluster theory (CCSD and CCSD(T)). The results from these calculations are presented in the Supporting Information. None of the results obtained by these computationally expensive methods was conclusively more reliable than the B3LYP results. This negative result with respect to the wave function based methods is simply due to the slow convergence of electronic energies as a function of both basis set and theoretical treatment of electron correlation. Although it is possible in principle to converge the electronic energy to within a few kilojoules per mole from the true value using CCSD(T), this becomes practically impossible even for the benzoquinones, which are the smallest molecules in the present study. The number of basis functions that are needed for convergence of the coupled cluster calculations leads to disk requirements (350−700 GB, depending on molecular symmetry), which are difficult to meet today. Accurate coupled cluster calculations on the reduction of anthraquinone would require at least 8.5 TB of disk space, in addition to the very time-consuming computations. On the basis of these difficulties in converging the wave function based methods with respect to basis functions, only B3LYP results are presented in this work.

The GAUSSIAN 98 and GAUSSIAN 03 program packages were employed for the calculations.[54] Molecular structures were optimized and analytical Hessians were subsequently calculated for all the optimized geometries using B3LYP and the basis set used for the optimization. Besides structural information and vibrational spectra, data from the Hessians were used for the thermochemical calculations. The electronic energies of the stationary structures involved in a particular reaction were used to calculate the electronic reaction energy at 0 K ($\Delta_r E(0\ \mathrm{K})$). Reaction enthalpies at 0 K ($\Delta_r H(0\ \mathrm{K})$) were obtained by adding the zero-point vibrational energies of the reacting molecules. Standard reaction enthalpies ($\Delta_r H^\circ$) were then calculated by taking into account the corresponding translational, rotational, vibrational and electronic partition functions. The partition functions were also used to calculate the standard reaction entropy and therefore, the standard Gibbs energy of reaction at 298 K ($\Delta_r G^\circ$). A detailed description on the theoretical approach behind the thermodynamic calculations has been given by Ochterski.[55] All four values ($\Delta_r E(0\ \mathrm{K})$, $\Delta_r H(0\ \mathrm{K})$, $\Delta_r H^\circ$, and $\Delta_r G^\circ$) are reported in the tables in kilojoules per mole.

As explained above, the explicitly correlated wave function based methods were found to require as large basis sets as possible (e.g., 6-311+G(3df,3pd)) for converging the electronic energy. DFT calculations are known to be much less sensitive to the size of the basis set, and this allows for the use of small basis sets as long as some requirements are fulfilled. Most of the B3LYP calculations were performed using the 6-311+G(d,p) basis set.[56,57] This basis set includes polarization functions on all atoms and diffuse functions on C and O, which is expected

to be sufficient for the calculation of molecular geometries and reaction energies. The effects of changing the basis set were investigated in two ways. Severe problems with the convergence of the Kohn−Sham orbitals were encountered for some of the anthraquinone species. The problems were most severe when diffuse functions were included, as in the 6-311+G(d,p) basis set, and convergence was much better with the smaller 6-311G-(d,p) basis set. As a consequence, results from calculations using both basis sets are presented for most of the anthra- and phenanthrenequinones. This makes it possible to determine the effect of diffuse functions on reaction energies. Investigations of the basis set expansion up to 6-311+G(3df,3pd) were performed for the two benzoquinones. Results are presented in sections 3.1.1 and 3.2.1 for this basis set and the slightly smaller 6-311+G(2df,2pd) set.

Solvation by water was investigated using a polarized continuum model (PCM). Molecular structures were optimized in a model water medium using the IEF−PCM[58] method as implemented in the GAUSSIAN 03 package. Subsequently, analytical Hessians, Gibbs energies of reduction and standard potentials were calculated for the optimized structures.

2.3.2. Calculation of Standard Potentials from Quantum Chemical Gibbs Energy Data. Standard potentials ($E°$) were calculated from

$$E° = -\Delta_r G°/nF \quad (1)$$

$\Delta_r G°$ is the calculated Gibbs energy for the redox reaction:

$$\mathrm{Ox(aq)} + \frac{n}{2}\mathrm{H_2(g)} \rightarrow \mathrm{Red(aq)} \quad (2)$$

n is the number of electrons transferred per molecule of reactant Ox(aq), F is Faraday's constant and Ox(aq) and Red(aq) are the oxidized and reduced species, respectively. The calculation of the standard potential of an individual redox couple requires the determination of the Gibbs energy of formation for all reactants and products using quantum chemistry methods. In addition, the reducing equivalent must be modeled properly.

One commonly used alternative procedure is to model electrons and protons separately. The energy of the electron depends on which reference is used, vacuum or an electrode. Calculations of redox potentials using explicit electrons and solvated protons were recently performed by Namazian et al. for quinones as one of the methods used in ref 27. Anderson and co-workers discussed the relationship between results from such calculations with experimentally determined standard potentials.[59,60] In these investigations, the solvation energies of H^+ and OH^- were computed, rather than using literature values as was done for H^+ in ref 27. There are difficulties with the explicit modeling of the solvation of H^+ and OH^- when using a limited number of water molecules in the calculation.[59,60] The values of the calculated binding energies are strongly dependent on the basis set employed and also ambiguities in the way enthalpy and Gibbs energy contributions are taken into account.

The problems associated with a calculation of the thermodynamic properties of the solvated proton are illustrated by the differences that are observed when increasing the number of water molecules in the calculation and using an extended basis set. For example, the standard Gibbs energy of solvation calculated for the system $H^+ + n_wH_2O$ were −7.08, −8.34, −8.97, and −9.46 eV respectively for $n_w = 1$, 2, 3 and 4.[61] These values should be compared to the best current estimates of single ionic solvation for the proton of −11.447 eV.[62] Consequently, the convergence to bulk water is rather slow and great care must be taken when designing calculations that employ incomplete solvation models and can benefit from cancellation of errors.

To avoid ambiguities as mentioned above, the standard potentials of the overall cell reactions involving neutral species have been considered in the present work rather than the individual half-cell reactions. Since the reference for the measurement of standard potentials is the hydrogen electrode (SHE), the use of the overall reaction with $H_2(g)$ limits the need to model charged species in solution. It is not possible, however, to eliminate all ionic species that appear in electrochemical reactions by this approach and it becomes necessary to incorporate acid/base equilibria and charged species into the model for calculations of potentials as functions of pH. By applying standard conditions, i.e., $a_{H+} = 1$, all weak acids appear in their neutral forms. However, the substantial ionicity of the solvent under these conditions is not explicitly included in the models used.

3. Results and Discussion

The reduction reactions of six different parent quinones, the *p*- and *o*- derivatives of benzo- and naphthoquinone, 9,10-anthraquinone, and 9,10-phenanthrenequinone, have been investigated. 1,4-BQ, 1,4-NQ, and 9,10-AQ denote the *p*-quinones, while 1,2-BQ, 1,2-NQ, and 9,10-PQ denote the *o*-quinones. Reduction reactions via semiquinone intermediates were also studied. Only reactions involving neutral species as reactants and products have been considered.

Figures 1, 2, 4, and 5 depict the optimized structures of the molecules studied, together with selected bond lengths, enthalpies and Gibbs energies of reduction at the B3LYP/6-311+G-(d,p) level of theory. Conformational isomers with respect to the orientation of the OH groups were investigated for 1,4-H_2-BQ and 1,4-H_2NQ. While the cis (**2**) and trans (**3**) isomers are energetically degenerate for hydrobenzoquinone, the cis (**6**) form is favored over the trans (**5**) conformation for 1,4-H_2NQ. This is a consequence of the repulsion between the H atoms in the OH and C−H groups, which is balanced by the attraction between the lone pair on the O atom and the C−H group. In 1,4-H_2NQ, the asymmetry caused by the side-ring allows the latter interaction to dominate. Consequently, only the trans form (**8**) was investigated for 9,10-H_2AQ, since the symmetrical positioning of the side-rings results in repulsion between the C−H and OH groups analogous to that observed for 1,4-H_2-BQ. Similarly to the 1,4-H_2BQ molecule, the cis and trans isomers are considered degenerate for 9,10-H_2AQ. The most stable conformational isomers of the quinols were used in these calculations.

Basis set expansions were found to alter bond distances in both quinones and quinols by less than 0.01 Å. This effect is too small to affect any trends. Consequently, the following discussion concerns bond distances calculated using the 6-311+G-(d,p) basis set, for which data are available for all the investigated molecules. All *p*-quinols have C−O bond distances between 1.35 and 1.39 Å, which are typical bond lengths for phenols.[63] An aliphatic alcohol usually has a longer (1.42 Å) C−O bond distance.[63] The shorter C−O bond length in a phenol results from electron donation from the nonbonding electron pair on O to the aromatic π-system of the carbon framework. Electron donation increases the strength of the C−O bond, and thus the OH group of the hydroquinone becomes more tightly bonded to the carbon framework compared with the hydroxyl group of an aliphatic alcohol. All *p*-quinones have very similar C═O bond lengths (1.21−1.22 Å), while the bonds in the central

TABLE 2: Calculated Thermodynamic Functions for the Gas Phase Reduction of *p*-Quinones To Yield the Corresponding Quinols[a,b]

	Δ_rE(0 K)	Δ_rH(0 K)	$\Delta_rH°$	$\Delta_rG°$(calc)	$\Delta_rG°$(corr)
1,4-BQ(g) + H_2(g) → *cis*-1,4-H_2BQ(g)	−161.5	−126.7	−133.6	−98.6	
→ *trans*-1,4-H_2BQ(g)	−162.0	−127.1	−134.1	−99.0	−107.3
	−168.0[c]	−133.0[c]	−140.0[c]	−104.7[c]	
	−167.4[d]	−132.4[d]	−139.6[d]	−104.0[d]	
1,4-NQ(g) + H_2(g) → *trans*-1,4-H_2NQ(g)	−107.1	−73.8	−80.3	−45.8	
→ *cis*-1,4-H_2NQ(g)	−112.6	−79.7	−86.0	−50.0	−63.5
	−118.5[c]	−84.6[c]	−91.5[c]	−54.3[c]	
9,10-AQ(g) + H_2(g) → *trans*-9,10-H_2AQ(g)	−29.7[e]	+0.8[e]	−4.9[e]	+30.1[e]	
	−37.7	−5.9	−12.0	+22.3	+8.8

[a] 1,4-BQ = 1,4-benzoquinone; 1,4-NQ = 1,4-naphthoquinone and 9,10-AQ = 9,10-anthraquinone. The symbols used have been defined in the text. All thermodynamic functions are given in kJ mol^{-1}. [b] Notes: B3LYP and the 6-311+G(d,p) basis set were used except as indicated. See sections 2.3.1 and 3.1.1 for discussions on basis set effects. [c] B3LYP and the 6-311+G(2df,2pd) basis set. [d] B3LYP and the 6-311+G(3df,3pd) basis set. [e] B3LYP and the 6-311G(d,p) basis set.

C_6-ring display significant variations. The four C−C single bonds next to the C═O groups have bond lengths between 1.48 and 1.49 Å, while the remaining two are either double bonds (1.34 Å) or aromatic bonds (1.41 Å). 1,4-BQ (**1**) has two double bonds, 1,4-NQ (**4**) one double bond and one aromatic bond, and 9,10-AQ (**7**) two aromatic bonds. The fact that different bond types are found for each of the parent *p*-quinones is important for understanding the trends in enthalpies and Gibbs energies of reduction to the quinols.

The few standard enthalpies of formation reported in the literature are indicated in the text. No Gibbs energy of formation or entropy data could be found in the literature for any of the compounds studied.

3.1. Calculation of Thermodynamic Functions for the Reduction of *p*-Quinones.

3.1.1. Reduction Reactions Yielding Hydroquinones. Table 2 shows the results for the calculations for the reaction Q(g) + H_2(g) → H_2Q(g). All four thermodynamic functions (Δ_rE(0 K), Δ_rH(0 K), $\Delta_rH°$, and $\Delta_rG°$—see section 2.3.1) are presented to show the various contributions to the reaction enthalpies and Gibbs energies. The trends observed are similar for all the quinones investigated. Zero-point energies add 31−35 kJ/mol to the electronic reaction energies (Δ_rE(0 K)), whereas the effect of temperature on reaction enthalpies lowers the value of Δ_rH(0 K) by 6−7 kJ/mol. Thus, the standard enthalpies are 26−28 kJ/mol more positive than Δ_rE(0 K). At 298 K, the entropy of reaction adds a further 34−36 kJ/mol to $\Delta_rH°$. In total, 60−63 kJ/mol have to be added to the electronic energies at 0 K in order to obtain the standard Gibbs energies of reaction. These contributions are substantial and therefore, Δ_rE(0 K) is not a good measure of the thermodynamic feasibility of these reactions. Importantly, the effects on the thermodynamic contributions to Δ_rE(0 K) from changing the size of the basis set are generally less than 1.5 kJ/mol. The details of basis set effects on the calculated values for Δ_rE(0 K) in particular are discussed in the following paragraph.

The convergence of the calculated thermodynamic functions with increasing size of the basis set was investigated in detail for the 2 e^-, 2 H^+ reduction of 1,4-BQ and in particular the addition of polarization functions to the 6-311+G(d,p) basis set. While the effect on Δ_rE(0 K) of expanding the basis set was found to be more than 20 kJ/mol for the explicitly correlated MP2 method, the effect is limited to 6 kJ/mol for B3LYP. This is expected since a large number of polarization functions are needed for the accurate description of electron correlation in methods such as MP2 and CCSD(T), while DFT methods are much less sensitive to the size of the basis set (see Supporting Information). The explicitly correlated methods and B3LYP display the same trend of increased stabilization of the quinol by the basis set expansion as compared with the quinone. This in turn makes the Δ_rE(0 K) values more negative. In general, most basis set effects were covered by using the 6-311+G(2df,2pd) basis set, while an increase to the larger 6-311+G(3df,3pd) basis set altered Δ_rE(0 K) by less than 1 kJ/mol for B3LYP. Other combinations of polarization functions were also investigated, mainly by using fewer functions for the H atoms. However, it was found that the additional polarization functions on the H atoms are particularly important for converging the energy. The reaction energy increases by 5 kJ/mol for the reduction of 1,4-NQ, when the 6-311+G(2df,2pd) basis set is used. The magnitude of this basis set effect is consistent with that observed for 1,4-BQ. However, since the basis set effect beyond 6-311+G(d,p) appears to be fairly constant, it can be easily corrected for in the calculations of the thermodynamic functions.

Diffuse functions were included in the basis sets used for 1,4-BQ and 1,4-NQ, i.e., 6-311+G(d,p), but the reduction of 9,10-AQ was also investigated using the 6-311G(d,p) basis set. This was due to difficulties with the convergence of the Kohn−Sham wave function used in DFT for reduced species related to 9,10-AQ (see section 2.3.1). The inclusion of diffuse functions lead to a stabilization of the quinol form by 7−8 kJ/mol with respect to the quinones for all the thermodynamic functions calculated. On the basis of this, it was estimated that diffuse functions makes all calculated thermodynamic functions 3−4 kJ/mol more negative (for some reactions and functions less positive) when one OH group is formed (e.g., the neutral semiquinone) and 7−8 kJ/mol more negative when two OH groups are formed.

Table 2 shows a clear trend in the thermodynamic functions for the reduction of the *p*-quinones. As the number of aromatic bonds in the central C_6-ring of the quinone increases, the enthalpies and Gibbs energies of reduction decrease. The comparisons below are based on the results obtained using the 6-311+G(d,p) basis set, for which data are available for all three reactions. While the reduction of 1,4-BQ is distinctly exothermic ($\Delta_rH° = -134$ kJ/mol) and spontaneous ($\Delta_rG° = -99$ kJ/mol), the reaction becomes barely exothermic ($\Delta_rH° = -12$ kJ/mol) and nonspontaneous ($\Delta_rG° = +22$ kJ/mol) for 9,10-AQ in the gas-phase. The values for the reduction of 1,4-NQ are intermediate ($\Delta_rH° = -86$ kJ/mol and $\Delta_rG° = -50$ kJ/mol). As discussed above, this trend arises mainly from changes in the electronic reaction energy Δ_rE(0 K).

Experimental values for the standard reduction enthalpies are $\Delta_rH° = -142.4$ kJ/mol[63] for 1,4-BQ and $\Delta_rH° = -99.5$ kJ/mol[64,65] for 1,4-NQ. The present calculations using the 6-311+G(d,p) basis set (Table 2) underestimate the reaction enthalpy by 8.3 kJ/mol for 1,4-BQ and by 13.5 kJ/mol for 1,4-NQ. A

TABLE 3: Calculated Differences in the Gibbs Energies of Solvation (kJ/mol) and Gibbs Energies of Reaction (kJ/mol) for the Reduction of *p*-Quinones in Water, Together with the Calculated Standard Potentials (V) for the 2-e$^-$ Reduction of the *p*-Quinones; $a_H+ = 1$[a]

	$\Delta_rG°_{solv}$	$\Delta_rG°_{aq}$(calc)	$\Delta_rG°_{aq}$(corr)	$E°$(calc)	$E°$(corr)	$E°$(exp)
1,4-BQ(aq) + H_2(g) → *trans*-1,4-H_2BQ(aq)	−26.6	−125.6	−133.9	0.651	0.694	0.6990 ± 0.001
1,4-NQ(aq) + H_2(g) → *cis*-1,4-H_2NQ(aq)	−27.0	−77.0	−90.5	0.399	0.469	0.470 ± 0.002
9,10-AQ(aq) + H_2(g) → *trans*-9,10-H_2AQ(aq)	−23.1	−0.8	−14.3	0.004	0.074	0.09 ± 0.03

[a] Notes: B3LYP, 6-311+G(d,p) basis set and the IEF−PCM method were used. Gibbs energies were obtained by using optimized molecular geometries and Hessians of the solvated species in water. $E°$(calc) is the standard potential for the uncorrected Gibbs energies, $E°$(corr) is that for the Gibbs energies corrected as described in sections 3.1.1 and 3.1.2 and $E°$ (exp) are the most reliable experimental values (see section 2.2 and Table 1).

TABLE 4: Calculated Gibbs Energies of Solvation (kJ/mol) for the Individual Species Involved in the Reduction of *p*-Quinones in Water[a]

	$\Delta G°_{solv}$		$\Delta G°_{solv}$		$\Delta G°_{solv}$
1,4-BQ(g) → 1,4-BQ(aq)	−31.4	1,4-NQ(g) → 1,4-NQ(aq)	−25.8	9,10-AQ(g) → 9,10-AQ(aq)	−19.4
1,4-HBQ(g) → 1,4-HBQ(aq)	−58.5	1,4-HNQ(g) → 1,4-HNQ(aq)	−52.8	9,10-HAQ(g) → 9,10-HAQ(aq)	−40.5
trans-1,4-H_2BQ(g) → *trans*-1,4-H_2BQ(aq)	−58.0	*cis*-1,4-H_2NQ(g) → *cis*-1,4-H_2NQ(aq)	−52.8	*trans*-9,10-H_2AQ(g) → *trans*-9,10-H_2AQ(aq)	−42.6

[a] Notes: B3LYP, the 6-311+G(d,p) basis set and the IEF−PCM method were used.

substantial part of this error is due to the limited number of basis functions, whereby the underestimate of $\Delta_rH°$ is reduced to 4.2 kJ/mol for 1,4-BQ and 8.0 kJ/mol for 1,4-NQ using the 6-311+G(2df,2pd) basis set (Table 2). At basis set convergence, both values fall within the average 9.3 kJ/mol error[52] of the B3LYP method. This error is due to the inexactness of the exchange-correlation functional in B3LYP.[52]

It appears reasonable to assume that the calculated $\Delta_rH°$ value for 9,10-AQ is underestimated by a similar amount (i.e., 13.5 kJ/mol), as was found for 1,4-NQ. This correction compensates for both the basis set incompleteness and the methodological error. The rationale for this approach is the fact that similar reduction reactions are considered. Corrected Gibbs energies for the reduction reaction, $\Delta_rG°$(corr), using the corrections to the B3LYP/6-311+G(d,p) enthalpies (−8.3 kJ/mol for 1,4-BQ and −13.5 kJ/mol for 1,4-NQ and 9,10-AQ), are given in Table 2. An important result is that in contrast to 1,4-BQ and 1,4-NQ, the reduction of 9,10-AQ is not spontaneous in the gas-phase.

The above corrections were employed to all reactions below, and both corrected (corr) and uncorrected (calc) values are given in Tables.

3.1.2. Calculation of Gibbs Energies of Solvation and Standard Potentials. Solvation was taken into account for the calculations of the Gibbs energy of reaction ($\Delta_rG°_{aq}$) and standard potentials ($E°$) in water. The calculations were carried out with molecules optimized using the IEF−PCM model as described in section 2.3.1 and the results are shown in Table 3. In addition, Table 3 shows the differences in Gibbs energies of solvation between reactants and products ($\Delta_rG°_{solv}$) calculated by subtracting the $\Delta_rG°$ values in water from those obtained in the gas phase (from Table 2). The Gibbs energies of solvation ($\Delta G°_{solv}$) for each of the molecules investigated are shown in Table 4. Standard potentials were calculated both from the $\Delta_rG°_{aq}$ values ($E°$(calc)) and from the corrected $\Delta_rG°$ values given in Table 1 and from $\Delta_rG°_{solv}$ ($E°$(corr)) and the standard potentials are compared with experimental data. Although there is some uncertainty in the exact value of $E°$(exp) for anthraquinone (see section 2.2 and Table 1), the agreement between calculated and experimental values is very good.

The $\Delta_rG°_{solv}$ values, which compare the reaction in the gas phase and in water, are similar for the three quinones, and fall between −23 and −27 kJ/mol. These negative values reflect the higher solvation energy of the C−OH group compared with C═O and their similarity is due to the presence of the same polar groups in this sequence. The calculated Gibbs energy of solvation of the individual quinones (Table 3) decreases from −31 kJ/mol for 1,4-BQ to −26 kJ/mol for 1,4-NQ and to −19 kJ/mol for 9,10-AQ. This trend is expected considering the increased hydrophobic character of these molecules due to the presence of aromatic side rings in both the oxidized and reduced forms of 1,4-NQ and 9,10-AQ.

The calculated $E°$(corr) value for 1,4-BQ is 0.694 V using the IEF−PCM solvation model. This is close to the well-determined experimental value 0.6990 ± 0.001 V at pH = 0 (see section 2.2). The result validates the corrections to the values of $\Delta_rG°$ in the gas-phase previously discussed. For the reduction of 1,4-NQ, $E°$(corr) is 0.469 V, which compares very well with the experimental value of 0.470 ± 0.002 V. The calculated $E°$(corr) for 9,10-AQ is 0.074 V. There is a scarcity of reliable literature values for this quinone and an average value of 0.09 ± 0.03 V was determined in section 2.2 as the best experimental estimate for $E°$(exp). The corrected potential falls within the error bars of $E°$(exp). It is concluded that all three $E°$(corr) values are within the error bars of $E°$(exp) or a few millivolts below (4 mV for 1,4-BQ) the experimental potentials. The error is thus much smaller than the uncertainty of the B3LYP method, as the deviation observed for 1,4-BQ corresponds to less than 1 kJ/mol error in the $\Delta_rG°_{aq}$ values.

3.1.3. Reduction Reactions Yielding *p*-Semiquinones. A general feature of all the semiquinones investigated is that while an electron is symmetrically delocalized in the conjugated system of the semiquinone radical anion, the inclusion of the proton in the molecule breaks this symmetry and localizes the electron onto one of the C═O groups. Although there are several sites available for proton binding, the present investigation focuses on those relevant to the formation of the dihydroquinone, i.e., protonation at one of the C═O moieties.

The molecular structure of all the semiquinones, 1,4-HBQ, 1,4-HNQ, and 9,10-HAQ (Figure 2, **9**, **10**, and **11**, respectively), display structural features intermediate between those of a quinone and a quinol. The C−C and C−O bonds can only be partially classified as single, double or aromatic since the bond lengths are between those typical for each bond type. This reflects the transformation of the conjugated π-system in the quinone to the aromatic hydroquinones on reduction. The structure of the neutral semiquinone of 9,10-AQ (**11**, Figure 2) displays a small imaginary vibrational frequency (41*i* cm^{-1}) at the B3LYP/6-311+G(d,p) level of theory, indicating that the potential energy surface (PES) is very flat. No energy minimum

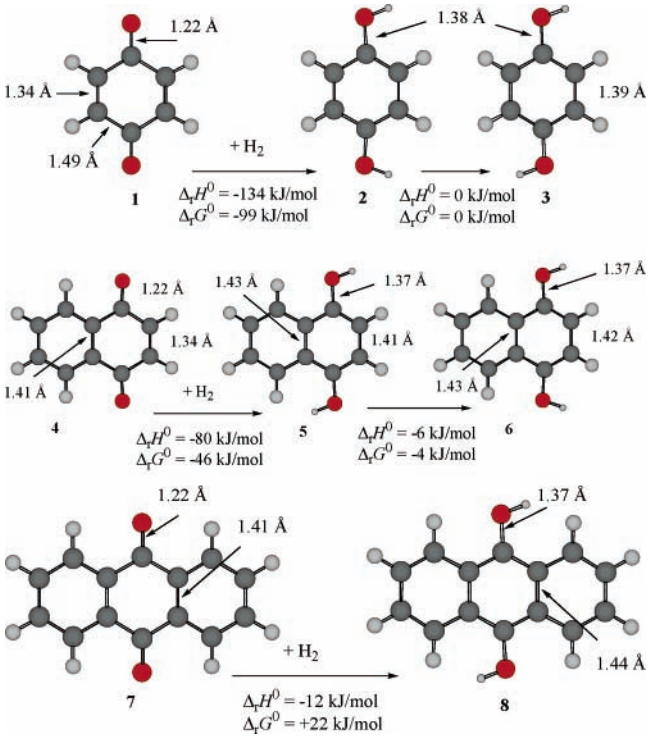

Figure 1. Optimized structures of the three *p*-quinones and the corresponding *p*-quinols (dihydroquinones). The values of $\Delta_r H°$ and $\Delta_r G°$ for the reduction reactions and for some selected bond lengths are shown. Results were obtained using B3LYP/6-311+G(d,p). 1,4-benzoquinone (**1**), *cis*-1,4-hydrobenzoquinone (**2**), *trans*-1,4-hydrobenzoquinone (**3**), 1,4-naphthoquinone (**4**), *trans*-1,4-hydronaphthoquinone (**5**), *cis*-1,4-hydronaphthoquinone (**6**), 9,10-anthraquinone (**7**), and 9,-10-hydroanthraquinone (**8**).

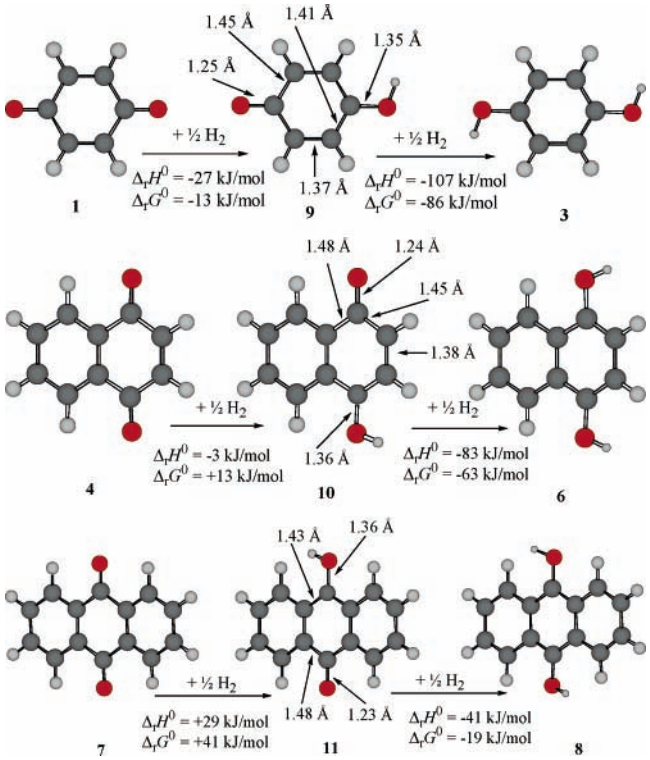

Figure 2. Optimized structures of neutral *p*-semiquinones (monohydroquinones), shown together with the corresponding quinones and quinols. The values of $\Delta_r H°$ and $\Delta_r G°$ for the two reduction steps and for some selected bond lengths are shown. Results were obtained using B3LYP/6-311+G(d,p). 1,4-semibenzoquinone (**9**), 1,4-seminaphthoquinone (**10**), and 9,10-semianthraquinone (**11**).

could be located for the semiquinone structure using this basis set. Without the addition of diffuse functions to the 6-311G-(d,p) basis set, the conformation calculated represents a true energy minimum on the PES since all vibrational frequencies are real. The structure contains one phenolic[48] (1.36 Å) and a C═O group (1.23 Å). The bond lengths of the four C−C bonds proximal to these two groups (1.43 and 1.48 Å, respectively) are between typical aromatic and single bonds. This is consistent with the features observed for the semiquinones of the two smaller *p*-quinones. Table 5 summarizes the thermodynamic data calculated for the neutral semiquinones in the gas phase, while Table 6 contains the calculated Gibbs energies of reduction in water and the corresponding reduction potentials. Table 7 shows calculated Gibbs energies and potentials for the disproportionation reaction, in which two semiquinones produce one quinone and one quinol.

The neutral semiquinone is an unstable reduction intermediate in the 2 e^-, 2 H^+ reduction of 1,4-BQ, and this is reflected in the values of the corresponding Gibbs energies. While the formation of 1,4-HBQ in the first 1 e^- reduction step is both exothermic ($\Delta_r H° = -27$ kJ/mol) and spontaneous ($\Delta_r G° = -13$ kJ/mol), these values are significantly lower than those for the second reduction step ($\Delta_r H° = -107$ kJ/mol and $\Delta_r G° = -87$ kJ/mol). Consequently, the continued reduction of 1,4-HBQ to the quinol is thermodynamically favorable. Moreover, the thermodynamic functions of the second reduction step render the disproportionation reaction of 1,4-HBQ to be both exothermic and spontaneous ($\Delta_r H° = -80$ kJ/mol and $\Delta_r G° = -74$ kJ/mol). Calculations using the larger 6-311+G(2df,2pd) basis set (Table 4) show that none of these effects stem from basis set incompleteness. $\Delta_r H°$ and $\Delta_r G°$ are both lowered by 2 kJ/mol for the first reduction step and by 3 kJ/mol for the second step. The effect on energies and enthalpies from adding polarization functions is thus equally distributed over the two reduction steps.

A possible explanation for the instability toward disproportionation is the stabilization of the unpaired electron in the semiquinones compared with the other quinone oxidation states. While the aromaticity of the quinol ensures the stability of the additional two electrons compared to the quinone, conjugation effects are less effective in stabilizing odd electron systems such as the semiquinones. If the unpaired electron were allowed to delocalize over the entire π-system of the carbon framework, it would benefit from the conjugation of the quinone. This would be the situation for the unprotonated semiquinone radical anion. However, protonation of the radical anion in one of the C═O group forces the electron distribution to be more localized. This can be seen in, e.g., the Mulliken spin population analysis (not shown). The localization of the unpaired electron is thus the most likely cause for the instability of 1,4-HBQ.

Aqueous seminaphthoquinone displays the same problems of stability toward disproportionation as found for 1,4-HBQ. Although the formation of 1,4-HNQ from 1,4-NQ is slightly exothermic ($\Delta_r H° = -3$ kJ/mol), the process is not spontaneous ($\Delta_r G° = +13$ kJ/mol). As for 1,4-BQ, the largest fraction of the reduction energy is released at the second reduction step from 1,4-HNQ to 1,4-H_2NQ ($\Delta_r H° = -83$ kJ/mol and $\Delta_r G° = -63$ kJ/mol). Consequently, the thermodynamic functions for the disproportionation of two 1,4-HNQ to 1,4-NQ and 1,4-H_2-NQ becomes similar to those determined for 1,4-HBQ ($\Delta_r H° = -81$ kJ/mol and $\Delta_r G° = -76$ kJ/mol). It is concluded that this protonated semiquinone is an unstable reduction intermediate for the same reason as 1,4-HBQ.

An endothermic and nonspontaneous first step is observed ($\Delta_r H° = +26$ kJ/mol and $\Delta_r G° = +42$ kJ/mol, see Table 5)

TABLE 5: Calculated Thermodynamic Functions for the Gas Phase Reduction of *p*-Quinones To Yield the Corresponding Neutral Semiquinones, Where 1,4-BQ = 1,4-Benzoquinone, 1,4-NQ = 1,4-Naphthoquinone, and 9,10-AQ = 9,10-Anthraquinone[a]

	Δ_rE(0 K)	Δ_rH(0 K)	$\Delta_rH°$	$\Delta_rG°$(calc)	$\Delta_rG°$(corr)
1,4-BQ(g) + $^1/_2$ H_2(g) → 1,4-HBQ(g)	−39.0	−23.1	−27.1	−12.5	−16.1
	−41.5[b]	−25.6[b]	−29.7[b]	−15.1[b]	
1,4-HBQ(g) + $^1/_2$ H_2(g) → *trans*-1,4-H_2BQ(g)	−123.0	−104.0	−107.0	−86.5	−90.7
	−126.4[b]	−107.3[b]	−110.4[b]	−89.6[b]	
1,4-NQ(g) + $^1/_2$ H_2(g) → 1,4-HNQ(g)	−14.0	+1.0	−2.7	+13.2	+6.4
1,4-HNQ(g) + $^1/_2$ H_2(g) → *cis*-1,4-H_2NQ(g)	−98.6	−80.7	−83.3	−63.2	−70.0
9,10-AQ(g) + $^1/_2$ H_2(g) → 9,10-HAQ(g)	+22.7[c]	+35.3[c]	+32.8[c]	+45.4[c]	+35.3
	+18.2	+30.2	+25.8	+42.0	
9,10-HAQ(g) + $^1/_2$ H_2(g) → *trans*-9,10-H_2AQ(g)	−52.4[c]	−34.5[c]	−37.7[c]	−15.3[c]	−26.5
	−55.9	−36.2	−37.8	−19.7	

[a] Notes: B3LYP and the 6-311+G(d,p) basis set were used except as indicated. See sections 2.3.1, 3.1.1, and 3.1.3 for discussions on basis set effects. [b] B3LYP and the 6-311+G(2df,2pd) basis set. [c] B3LYP and the 6-311G(d,p) basis set.

TABLE 6: Calculated Differences in the Gibbs Energies of Solvation (kJ/mol) and Gibbs Energies of Reaction (kJ/mol) for the Reduction of *p*-Quinones via the Corresponding Semiquinones in Water, Together with the Calculated Standard Potentials (V) for the 1-e$^-$ Reduction Steps of the *p*-Quinones (a_{H^+} = 1)[a]

	$\Delta_rG°_{solv}$	$\Delta_rG°_{aq}$(calc)	$\Delta_rG°_{aq}$(corr)	$E°$(calc)	$E°$(corr)
1,4-BQ(aq) + $^1/_2$$H_2$(g) → 1,4-HBQ(aq)	−27.2	−39.7	−43.8	0.411	0.454
1,4-HBQ(aq) + $^1/_2$$H_2$(g) → *trans*-1,4-$H_2$BQ(aq)	+0.5	−86.0	−90.2	0.891	0.934
1,4-NQ(aq) + $^1/_2$$H_2$(g) → 1,4-HNQ(aq)	−27.0	−13.8	−20.5	0.143	0.213
1,4-HNQ(aq) + $^1/_2$$H_2$(g) → *cis*-1,4-$H_2$NQ(aq)	0.0	−63.2	−70.0	0.655	0.726
9,10-AQ(aq) + $^1/_2$$H_2$(g) → 9,10-HAQ(aq)	−21.1	+20.9	+14.2	−0.217	−0.147
9,10-HAQ(aq) + $^1/_2$$H_2$(g) → *trans*-9,10-$H_2$AQ(aq)	−2.1	−21.8	−28.5	0.226	0.295

[a] Notes: B3LYP, the 6-311+G(d,p) basis set and the IEF−PCM method was used in general. Gibbs energies obtained by using optimized molecular geometries and Hessians of the solvated species in water. $E°$ (calc) is the standard potential for the uncorrected Gibbs energies; $E°$(corr) is that for the Gibbs energies corrected as described in section 3.1.3.

TABLE 7: Calculated Gibbs Energies of Reaction (kJ/mol) for the Disproportionation of *p*-Semiquinones to the Quinone and Quinol in the Gas-Phase and in Water, together with the Calculated Standard Potentials (V)[a]

	$\Delta_rG°$	$\Delta_rG°_{aq}$	$E°$
2(1,4-HBQ(g)) → 1,4-BQ(g) + 1,4-H_2BQ(g)	−74.0		
2(1,4-HBQ(aq)) → 1,4-BQ(aq) + 1,4-H_2BQ(aq)		−46.3	0.240
2(1,4-HNQ(g)) → 1,4-NQ(g) + 1,4-H_2NQ(g)	−76.4		
2(1,4-HNQ(aq)) → 1,4-NQ(aq) + 1,4-H_2NQ(aq)		−49.4	0.256
2(9,10-HAQ(g)) → 9,10-AQ(g) + 9,10-H_2AQ(g)	−61.7		
2(9,10-HAQ(aq)) → 9,10-AQ(aq) + 9,10-H_2AQ(aq)		−42.7	0.221

[a] Notes: Values were calculated using data from Tables 4 and 5.

for the formation of 9,10-HAQ using the 6-311+G(d,p) basis set. At the same level of theory, values of $\Delta_rH° = -38$ kJ/mol and $\Delta_rG° = -20$ kJ/mol are obtained for the reduction of 9,-10-HAQ to the quinol. The use of diffuse functions results in a 4 kJ/mol stabilization of the reduced forms for each 1 e$^-$ step, i.e., half the basis set effect observed for the overall 2 e$^-$ reduction. The thermodynamic functions for the reduction of 9,10-AQ to 9,10-HAQ are approximately 30 kJ/mol more positive than those for the first reduction step on 1,4-NQ. The values are 40−45 kJ/mol more positive for the second reduction step. The Gibbs energy change for the second reduction step is smaller for 9,10-AQ than for 1,4-NQ or 1,4-BQ. This does not alter the thermodynamic functions for the disproportionation reaction, which is similar to that of the smaller *p*-quinones ($\Delta_rH° = -64$ kJ/mol and $\Delta_rG° = -62$ kJ/mol for 2 9,10-HAQ → 9,10-AQ + 9,10-H_2AQ).

In the absence of experimental data on the heats of formation for any of the semiquinones, it is not possible to verify the quality of the calculated thermodynamic functions. However, the overall standard reduction enthalpy for 1,4-BQ is underestimated by 8.3 kJ/mol compared to experimental data (section 3.1.1). A reasonable guess is that this deviation is equally distributed over the two 1 e$^-$, 1 H^+ reduction steps via 1,4-HBQ, i.e., 4.15 kJ/mol for each step. The underestimate was found to be slightly larger (13.5 kJ/mol) for the reduction of 1,4-NQ to the corresponding quinol and this value was also used for the 2 e$^-$, 2 H^+ reduction of 9,10-AQ. Consequently, an enthalpy underestimate of 6.75 kJ/mol for each step in the reduction via 1,4-HNQ and 9,10-HAQ can be assumed. Values for $\Delta_rG°$ corrected in this way are shown in Table 5. These corrections do not change the conclusion that the protonated semiquinones are unstable reduction intermediates for the three *p*-quinones in the gas phase.

The calculated Gibbs energies of reduction in water ($\Delta_rG°_{aq}$) were calculated as described in section 2.2.1 and the results are shown in Table 5. These values were used for calculating the differences in Gibbs energies of solvation ($\Delta_rG°_{solv}$) and standard potentials ($E°$(calc)) for the Q/QH$^\bullet$ and QH$^\bullet$/QH_2 couples. Corrected potentials ($E°$(corr)) were calculated based on the corrections to $\Delta_rG°$ in Table 5, i.e., assuming that the energy underestimate from the calculations is equally distributed over the two redox couples. A comparison of all calculated $E°$(corr) values are shown in Figure 3. The Gibbs energies of solvation ($\Delta G°_{solv}$) for each of the semiquinones are shown in Table 4.

The stabilization by solvation of the semiquinones is similar to that of the quinols (section 3.1.2). The total changes in $\Delta_rG°_{solv}$ are 23−27 kJ/mol for the three *p*-quinones and most of the energy changes result from the first reduction step Q/QH$^\bullet$. Although most of the solvation energy gain applies to the first redox couple, formation of the neutral semiquinone is less favorable than that for the reduction to the quinol. This has notable consequences on the $\Delta_rG°_{aq}$ values for the dispropor-

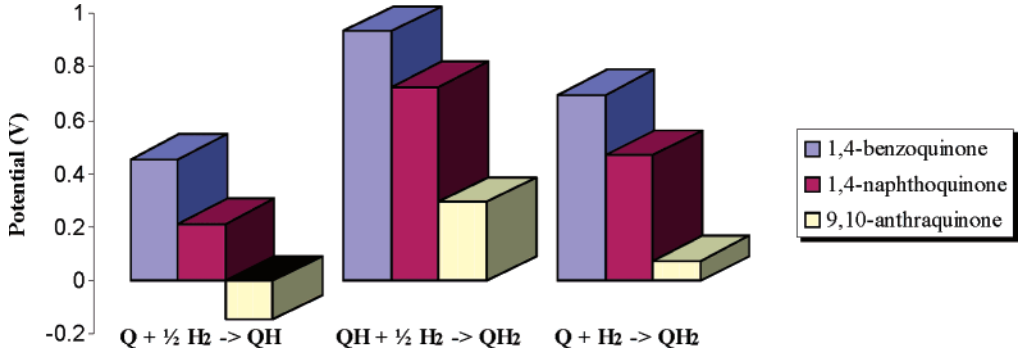

Figure 3. Calculated and corrected values ($E°$(corr)) for the reduction reactions Q + $^1/_2H_2$ → QH, QH + 1/2 H_2 → QH_2 and Q + H_2 → QH_2 for the three *p*-quinones.

tionation reactions (1,4-HBQ, −46 kJ/mol; 1,4-HNQ, −49 kJ/mol; 9,10-HAQ, −43 kJ/mol), which are lower than the gas-phase energies. However, disproportionation remains spontaneous. It can be noted that the Gibbs energies are very similar for the three *p*-semiquinones at pH = 0.

The corrected potentials calculated are probably the best estimates available for the stepwise reduction of *p*-quinones at pH = 0. All the calculated and corrected potentials for the Q/QH• couple in Table 6 are significantly less positive than those determined for the QH•/QH_2 couple, which is illustrated by the patterns in Figure 3. The difference in the $E°$ values for the two couples are fairly similar for the three *p*-quinones and corresponds to the doubled potentials for the disproportionation reactions (1,4-BQ, 0.24 V; 1,4-NQ, 0.26 V; 9,10-AQ, 0.22 V).

3.2. Calculation of the Thermodynamic Functions for the Reduction of *o*-Quinones.

3.2.1. Reduction Reactions Yielding Quinols and Their Standard Potentials. The structures of the *o*-quinones are displayed in Figure 4. Three of the four C−C single bonds in the central C_6-ring have bond lengths between 1.47 and 1.48 Å and the remaining two bonds in the ring have either double (1.35 Å) or aromatic (1.41 Å) bond character. 1,2-BQ (**12**) has two double bonds, 1,2-NQ (**14**) one double bond and one aromatic bond, and 9,10-PQ (**16**) two aromatic bonds. Thus, the *o*-quinones are very similar to the corresponding *p*-compounds. There is, however, one significant difference in the length of the C−C bond that connects the two carbonyl groups, which is greater (1.55−1.57 Å) than that of the other three single bonds. The increased length is due to electrostatic repulsion between the neighboring C═O units. This arises from the partial positive charge on the two C atoms, as well as from the interactions between the π-electrons and the lone-pairs of the two C═O groups. The elongation of the C_1-C_2 (C_9-C_{10}) bonds in the *o*-quinones, as compared to the *p*-quinones, affects the enthalpy and Gibbs energy of reduction. The thermodynamic functions for the reaction Q(g) + H_2(g) ↔ H_2Q(g) are shown in Table 8. The computed values for the standard Gibbs energies of reaction for the 2 e^-, 2 H^+ reduction of *o*-quinones are found to be 64−66 kJ/mol more positive than the Δ_rE(0 K) values, which is remarkably similar to that observed for the *p*-quinones.

All the *o*-quinols investigated, 1,2-H_2BQ (catechol) (**13**), 1,2-H_2NQ (**15**), and 9,10-H_2PQ (**17**), have the OH groups oriented in a syn conformation (Figure 4). The syn orientation optimizes intramolecular interactions, although the resulting hydrogen bond between the two OH groups is rather weak. This is shown by the distances of the interconnecting O−H bonds, which are between 2.14 and 2.15 Å for the three *o*-quinols. Two different C−O bond lengths are observed in each of the quinol molecules. The longer C−O bond is found for the COH group, which is the acceptor for the hydrogen bond from the other COH group.

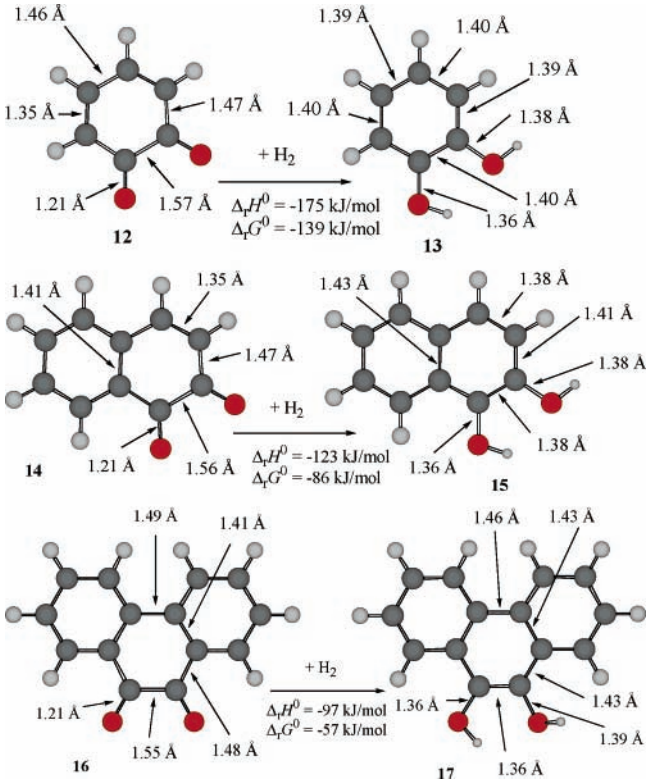

Figure 4. Optimized structures of the three *o*-quinones and the corresponding *o*-quinols (dihydroquinones). The values of $\Delta_rH°$ and $\Delta_rG°$ for the reduction reactions and for some selected bond lengths are shown. Results obtained using B3LYP/6-311+G(d,p). 1,2-benzoquinone (**12**), 1,2-hydrobenzoquinone (**13**), 1,2-naphthoquinone (**14**), 1,2-hydronaphthoquinone (**15**), 9,10-phenanthrenequinone (**16**), and 9,10-hydrophenanthrenequinone (**17**).

Similarly to the *p*-quinols, the C−O bond lengths in *o*-quinols (1.36−1.39 Å) are typical for phenols. These bonds are shorter than those found in alcohols due to electron donation from the nonbonding electron pair on the O into the aromatic π-system. A shortening of the C_1-C_2 (C_9-C_{10}) bond length on reduction, which is specific to the *o*-quinones, is observed. The resulting bond lengths (1.36−1.40 Å) can be classified as aromatic.

Table 8 indicates a similar trend in the reduction energetics as previously discussed for the *p*-quinones (cf. Table 2). Yet, although $\Delta_rH°$ and $\Delta_rG°$ decrease in the sequence 1,2-BQ, 1,2-NQ, and 9,10-PQ, i.e., as the number of aromatic bonds in the quinone central C_6-ring increases, the decrease is much smaller for the *o*-quinones compared with the *p*-quinones (i.e., in the sequence 1,4-BQ, 1,4-NQ, and 9,10-AQ). The values of the thermodynamic functions for reduction are higher for the *o*-quinones than for the *p*-quinones (∼40 kJ/mol for BQ and

TABLE 8: Calculated Thermodynamic Functions for the Gas Phase Reduction of *o*-Quinones To Yield the Corresponding Quinols[a,b]

	$\Delta_r E$(0 K)	$\Delta_r H$(0 K)	$\Delta_r H°$	$\Delta_r G°$(calc)	$\Delta_r G°$(corr)
1,2-BQ(g) + H_2(g) → 1,2-H_2BQ(g)	−203.6	−167.6	−174.8	−139.0	−147.3
	−210.2[c]	−173.3[c]	−181.0[c]	−143.9[c]	
	−209.3[d]	−172.3[d]	−180.1[d]	−142.6[d]	
1,2-NQ(g) + H_2(g) → 1,2-H_2NQ(g)	−150.3	−116.1	−122.9	−86.0	−99.5
9,10-PQ(g) + H_2(g) → 9,10-H_2PQ(g)	−117.1[e]	−82.9[e]	−90.1[e]	−51.8[e]	
	−123.8	−89.6	−96.5	−57.1	−70.6

[a] 1,2-BQ = 1,2-benzoquinone, 1,2-NQ = 1,2-naphthoquinone and 9,10-PQ = 9,10-phenanthrenequinone [b] Notes: B3LYP and the 6-311+G(d,p) basis set were used except as indicated.See sections 2.3.1 and 3.2.1 for discussions on basis set effects. [c] B3LYP and the 6-311+G(2df,2pd) basis set. [d] B3LYP and the 6-311+G(3df,3pd) basis set. [e] B3LYP and the 6-311G(d,p) basis set.

TABLE 9: Calculated Differences in the Gibbs Energies of Solvation (kJ/mol) and Gibbs Energies of Reaction (kJ/mol) for the Reduction of *o*-Quinones in Water, together with the Calculated Standard Potentials (V) for the 2-e⁻ Reduction of the *o*-Quinones (a_H+ = 1)[a]

	$\Delta_r G°_{solv}$	$\Delta_r G°_{aq}$(calc)	$\Delta_r G°_{aq}$(corr)	$E°$(calc)	$E°$(corr)	$E°$(exp)
1,2-BQ(aq) + H_2(g) → 1,2-H_2BQ(aq)	−13.2	−152.2	−160.5	0.789	0.832	0.831 ± 0.016
1,2-NQ(aq) + H_2(g) → 1,2-H_2NQ(aq)	−8.8	−95.2	−108.7	0.493	0.563	0.547 ± 0.002
9,10-PQ(aq) + H_2(g) → 9,10-H_2PQ(aq)	−15.9	−73.0	−86.5	0.378	0.448	0.442 ± 0.002

[a] Notes: B3LYP, 6-311+G(d,p) basis set and the IEF−PCM method were used. Gibbs energies were obtained by using optimized molecular geometries and Hessians of the solvated species in water. $E°$(calc) is the standard potential for the uncorrected Gibbs energies, $E°$(corr) is that for the Gibbs energies corrected as described in section 3.2.1 and $E°$ (exp) is the most reliable experimental value in each case (see section 2.2 and Table 1).

NQ and ∼90 kJ/mol for AQ/PQ). This trend originates from differences in $\Delta_r E$(0 K), probably caused by the repulsion between the two neighboring C═O groups.

The relaxation of the O═C_1−C_2═O unit upon reduction can be assumed to account for the main fraction of the 40 kJ/mol reduction energy increase observed for 1,2-BQ and 1,2-NQ, as compared to 1,4-BQ and 1,4-NQ. It appears reasonable to assign a similar increase in the reduction energy of 9,10-PQ, as compared to 9,10-AQ, to the shortening of the C_9−C_{10} bond. However, the additional 50 kJ/mol increase in this comparison must be due to another effect, which is important for the larger quinones. An interesting structural feature in this context is the bond lengths of the aromatic C−C bonds in the two side rings. A larger range of bond distances is found for 9,10-H_2AQ (1.37−1.44 Å) than for 9,10-H_2PQ (1.38−1.42 Å). This difference indicates that the aromatic conjugation is more efficient in 9,10-H_2PQ than it is in 9,10-H_2AQ. No difference of this type is present in the two quinones (9,10-AQ and 9,10-PQ), which have the same bond distance ranges (1.39−1.41 Å). It is therefore reasonable to assume that the differences in aromaticity between the two quinols account for the additional reaction energy observed in the reduction of 9,10-PQ, as compared to the reduction of 9,10-AQ. One reason the aromatic system is more disturbed in 9,10-H_2AQ than it is in 9,10-H_2PQ is that the central locations of the C−OH groups in anthraquinol destroys the electronic conjugation between the side rings. In phenanthrenequinol, the unsubstituted C−C bond opposite to the two C−OH groups connects the side rings with each other. This allows for conjugation between the two side rings, which is energetically favorable. The effect of diffuse functions (i.e., the 6-311G(d,p) vs 6-311+G(d,p) basis sets) on the thermodynamic functions for the reduction of 9,10-PQ was a lowering by 5−7 kJ/mol. This effect is of similar magnitude as observed for 9,10-AQ.

No experimental values have been found for any of the quantities in Table 8. It is therefore not possible to obtain exact figures on the magnitude of errors, but it seems reasonable to assume that B3LYP underestimates reduction energies and enthalpies to a similar extent to those observed for the reduction of *p*-quinones. The effect of expanding the basis set with respect to the number of polarization functions was investigated for the reduction of 1,2-BQ. By employment of the 6-311+G(2df,2pd) basis set, $\Delta_r E$(0 K) was lowered by 7 kJ/mol and $\Delta_r H°$ by 6 kJ/mol (Table 8). The lowering was slightly smaller for the 6-311+G(3df,3pd) basis set (6 kJ/mol for $\Delta_r E$(0 K) and 5 kJ/mol for $\Delta_r H°$). These values are very similar to the basis set effects observed for the reduction of 1,4-BQ. The $\Delta_r G°$ values in Table 8, obtained directly from calculations (calc), were consequently corrected using the same corrections as were used for the *p*-quinones (−8.3 kJ/mol for the reduction of 1,2-BQ and −13.5 kJ/mol for the reductions of 1,2-NQ and 9,10-PQ). As previously discussed, the reason behind the corrections is that they compensate for both the basis set incompleteness at the 6-311+G(d,p) level and for the systematic inaccuracy of the B3LYP method. The similarity in the value of the corrections is a consequence of the similarity of the reactions compared. The corrected Gibbs energies are shown as $\Delta_r G°$(corr) in Table 8.

Gibbs energies of reaction ($\Delta_r G°_{aq}$) in water and standard potentials ($E°$) were calculated using the same methodology as for the *p*-quinones. Table 9 shows values obtained both directly from calculations ($\Delta_r G°_{aq}$(calc) and $E°$(calc)), and values that have been corrected as described above ($\Delta_r G°_{aq}$(corr) and $E°$(corr)). The changes in the Gibbs energies of solvation in the reduction reaction ($\Delta_r G°_{solv}$) are also presented in Table 9.

The calculated differences between the $\Delta_r G°_{solv}$ values are significantly lower for the *o*-quinones (9−16 kJ/mol) than for the *p*-quinones (23−27 kJ/mol). This is a result of the smaller change in solvation energy for the reduction of the *o*-quinone to *o*-quinol compared with the same process for *p*-quinone. The individual Gibbs energies of solvation ($\Delta G°_{solv}$) for the three *o*-quinones (Table 10) are similar to those obtained for the *p*-quinones. The observed difference between the $\Delta_r G°_{solv}$ values of the two quinone types is due to the low Gibbs energies of solvation for the *o*-quinols as compared to those of the *p*-quinols. This is probably the result of the weak intramolecular hydrogen bond in the *o*-quinols. One of the C−OH groups is thus less prone to interact with the solvent, which results in the observed reduction of the solvation energy.

The calculated $E°$(corr) value for the reduction of 1,2-BQ is 0.832 V. This result is within the error of the experimental potential (0.831 ± 0.016 V, see section 2.2 and Table 1), although there is considerable uncertainty in the $E°$(exp) value.

TABLE 10: Calculated Gibbs Energies of Solvation (kJ/mol) for the Species Involved in the Reduction of *o*-Quinones in Water[a]

	$\Delta G°_{solv}$		$\Delta G°_{solv}$		$\Delta G°_{solv}$
1,2-BQ(g) → 1,2-BQ(aq)	−31.3	1,2-NQ(g) → 1,2-NQ(aq)	−34.8	9,10-PQ(g) → 9,10-PQ(aq)	−23.1
1,2-HBQ(g) → 1,2-HBQ(aq)	−30.4	1,2-HNQ(g) → 1,2-HNQ(aq)	−29.9	9,10-HPQ(g) → 9,10-HPQ(aq)	−25.6
1,2-H_2BQ(g) → 1,2-H_2BQ(aq)	−44.5	1,2-H_2NQ(g) → 1,2-H_2NQ(aq)	−43.9	9,10-H_2PQ(g) → 9,10-H_2PQ(aq)	−39.0

[a] Notes: B3LYP, the 6-311+G(d,p) basis set and the IEF−PCM method were used.

TABLE 11: Calculated Thermodynamic Functions for the Reduction of *o*-Quinones To Yield the Corresponding Neutral Semiquinone[a,b]

	$\Delta_r E$(0 K)	$\Delta_r H$(0 K)	$\Delta_r H°$	$\Delta_r G°$(calc)	$\Delta_r G°$(corr)
1,2-BQ(g) + $^1/_2H_2$(g) → 1,2-HBQ(g)	−96.8	−78.4	−83.3	−64.8	−68.9
1,2-HBQ(g) + $^1/_2H_2$(g) → 1,2-H_2BQ(g)	−106.8	−89.2	−91.6	−74.2	−78.4
1,2-NQ(g) + $^1/_2H_2$(g) → 1,2-HNQ(g)	−64.6	−47.3	−51.7	−31.9	−38.6
1,2-HNQ(g) + $^1/_2H_2$(g) → 1,2-H_2NQ(g)	−85.7	−68.8	−71.2	−54.1	−60.9
9,10-PQ(g) + $^1/_2H_2$(g) → 9,10-HPQ(g)	−53.8[c]	−36.9[c]	−41.3[c]	−22.2[c]	−31.0
	−56.9	−40.6	−44.8	−24.3	
9,10-HPQ(g) + $^1/_2H_2$(g) → 9,10-H_2PQ(g)	−63.3[c]	−46.0[c]	−48.8[c]	−29.7[c]	−39.5
	−66.9	−49.1	−51.7	−32.8	

[a] 1,2-BQ = 1,2-benzoquinone; 1,2-NQ = 1,2-naphthoquinone and 9,10-PQ = 9,10-phenanthrenequinone [b] Notes: B3LYP and the 6-311+G(d,p) basis set were used except as indicated. (a) B3LYP and the 6-311G(d,p) basis set. See sections 2.3.1 and 3.2.1 for descriptions of the effects of diffuse functions on reaction energetics (stabilizing the lone-pairs on O in the C−OH units in 9,10-HPQ and 9,10-H_2PQ). [c] B3LYP and the 6-311G(d,p) basis set were used.

TABLE 12: Calculated Differences in the Gibbs Energies of Solvation (kJ/mol) and Gibbs Energies of Reaction (kJ/mol) for the Reduction of *o*-Quinones via the Corresponding Semiquinones in Water, Together with the Calculated Standard Potentials (V) for the 1-e$^-$ Reduction Steps of the *o*-Quinones ($a_H+ = 1$)[a]

	$\Delta_r G°_{solv}$	$\Delta_r G°_{aq}$(calc)	$\Delta_r G°_{aq}$(corr)	$E°$(calc)	$E°$(corr)
1,2-BQ(aq) + $^1/_2H_2$(g) → 1,2-HBQ(aq)	+1.0	−63.8	−67.9	0.662	0.704
1,2-HBQ(aq) + $^1/_2H_2$(g) → 1,2-H_2BQ(aq)	−14.1	−88.3	−92.5	0.915	0.959
1,2-NQ(aq) + $^1/_2H_2$(g) → 1,2-HNQ(aq)	+4.9	−27.0	−33.7	0.280	0.349
1,2-HNQ(aq) + $^1/_2H_2$(g) → 1,2-H_2NQ(aq)	−14.0	−68.1	−74.9	0.706	0.776
9,10-PQ(aq) + $^1/_2H_2$(g) → 9,10-HPQ(aq)	−2.5	−26.8	−33.5	0.278	0.347
9,10-HPQ(aq) + $^1/_2H_2$(g) → 9,10-H_2PQ(aq)	−13.3	−46.1	−52.9	0.478	0.548

[a] Notes: B3LYP, the 6-311+G(d,p) basis set and the IEF−PCM method were used. Gibbs energies obtained by using optimized molecular geometries and Hessians of the solvated species in water.

TABLE 13: Calculated Gibbs Energies of Reaction (kJ/mol) for the Disproportionation of *o*-Semiquinones to the Quinone and Quinol in the Gas-Phase and in Water, together with the Calculated Standard Potentials (V)[a]

	$\Delta_r G°$	$\Delta_r G°_{aq}$	$E°$
2(1,2-HBQ(g)) → 1,2-BQ(g) + 1,2-H_2BQ(g)	−10.0		
2(1,2-HBQ(aq)) → 1,2-BQ(aq) + 1,2-H_2BQ(aq)		−24.5	0.127
2(1,2-HNQ(g)) → 1,2-NQ(g) + 1,2-H_2NQ(g)	−22.2		
2(1,2-HNQ(aq)) → 1,2-NQ(aq) + 1,2-H_2NQ(aq)		−41.1	0.213
2(9,10-HPQ(g))) → 9,10-PQ(g) + 9,10-H_2PQ(g)	−8.5		
2(9,10-HPQ(aq))) → 9,10-PQ(aq) + 9,10-H_2PQ(aq)		−19.3	0.100

[a] Notes: Values were calculated using data from Tables 11 and 12.

The value is considerably higher than the calculated potentials presented previously in the literature, e.g., those obtained by Reynolds et al.[20] using MP2 and a quinone reference method. Although the difference is due to the use of an empirical correction in the present work, the $E°$(corr) value is supported by a critical evaluation of the $E°$(exp) value used in, e.g., ref 20 (see section 2.2.1.). The use of the correction is justified by the agreement of $E°$(corr) and $E°$(exp) for the two larger *o*-quinones. A value of 0.563 V has been calculated for the corrected reduction potential of 1,2-NQ, which is 14 mV more positive than the high end of the experimental range (0.547 ± 0.002 V). The error corresponds to a $\Delta_r G°_{aq}$(corr) value that is approximately 2.7 kJ/mol too negative. This could mean that the 13 kJ/mol correction is slightly too large, but importantly it shows that the correction has the right sign and magnitude. The $E°$(corr) value for the reduction of 9,10-PQ is 0.448 V, which is 4 mV more positive than the high end of the $E°$(exp) value. This deviation corresponds to an uncertainty of less than 1 kJ/mol in the $\Delta_r G°_{aq}$(corr) value for 9,10-PQ. The close agreement between the $E°$(corr) and $E°$(exp) values shows the usefulness of the systematic corrections to the $\Delta_r G°$ values.

3.2.2. Reduction Reactions Yielding *o*-Semiquinones. The thermodynamic functions for reductions in the gas phase are presented in Table 11. A comparison with to the results for the *p*-semiquinones indicates that the proximity of the C−OH group to the carbonyl group influences the enthalpies and Gibbs energies of reaction. Table 12 shows the calculated Gibbs energies of reduction in water and the corresponding reduction potentials using the same corrections as described for the *p*-quinones, and Table 13 presents $\Delta_r G°$ and $E°$ values for the disproportionation reactions.

Similar to the observation for *p*-semibenzoquinone, *o*-semibenzoquinone, 1,2-HBQ (**18**), displays structural parameters that are intermediate between those of the quinone and the corresponding quinol. There are however two important differences. The C−OH bond length (1.33 Å), is slightly shorter than in phenols and closer to that found for crystalline enols.[48] This is due to the interaction between the C−OH and C═O groups,

which can be described as a long hydrogen bond (The O−H bond distance between the two groups is 2.06 Å). The lengths of the other C−C and C−O bonds fall between those for single, double or aromatic bonds. The transformation of the π-system of the quinone to an aromatic ring in the quinol is more complete than for 1,4-HBQ. However, the shortening of the C_1-C_2 bond to 1.47 Å is more important for the reaction enthalpies and energies, as was discussed for the 2 e^-, 2 H^+ reduction in the previous section. The bond is shortened due to the lower repulsion between the carbonyls when one group is replaced by C−OH. Another effect of hydrogen bonding between the C−OH and C═O groups is that radical localization is minimized. This is contrary to what was found for 1,4-HBQ (see section 3.1.3). Consequently, the first 1 e^- reduction step becomes exothermic ($\Delta_rH° = -83$ kJ/mol) and spontaneous ($\Delta_rG° = -65$ kJ/mol), with values fairly similar to those for the second reduction step ($\Delta_rH° = -92$ kJ/mol and $\Delta_rG° = -74$ kJ/mol). The disproportionation of 1,2-HBQ is thus much less favored ($\Delta_rH° = -8$ kJ/mol and $\Delta_rG° = -10$ kJ/mol) than for the 1,4-HBQ counterpart.

Similar trends are observed for the reduction of 1,2-NQ to 1,2-HNQ (**19**). The C−OH bond distance (1.33 Å) is typical of an enol, while the lengths of the other bonds are less typical. The C_1-C_2 bond is shortened to 1.46 Å. The formation of 1,2-HNQ from 1,2-NQ is exothermic ($\Delta_rH° = -52$ kJ/mol) and spontaneous ($\Delta_rG° = -32$ kJ/mol). The values, however, are 19−22 kJ/mol more negative for the second reduction step ($\Delta_rH° = -71$ kJ/mol and $\Delta_rG° = -54$ kJ/mol), which is larger than for 1,2-HBQ. Consequently, the disproportionation of 1,2-HNQ is more favorable ($\Delta_rH° = -19$ kJ/mol and $\Delta_rG° = -22$ kJ/mol). The structure of the neutral semiquinone of 9,10-PQ (**20**) is shown in Figure 5, and the shortening of the C_9-C_{10} bond follows the trend observed for the other *o*-quinones. Both reduction steps are exothermic and spontaneous, but the difference in energy between the two steps is similar to those of 1,2-HBQ. The enthalpy and Gibbs energy for the disproportionation reaction are similar ($\Delta_rH° = -7$ kJ/mol and $\Delta_rG° = -9$ kJ/mol). It can be noted, that the addition of diffuse functions to the basis set lowered the thermodynamic function for the first reduction step on 9,10-PQ by 2 kJ/mol, and by 3 kJ/mol for the second step. The higher disproportionation energy and enthalpy for 1,2-HNQ compared to the other two *o*-semiquinones is observed already in the $\Delta_rE°$(0 K) values. The difference between the $\Delta_rE°$(0 K) values of the two reduction steps is approximately 10 kJ/mol larger for 1,2-NQ than for 1,2-BQ and 9,10-PQ. The effect is thus due to different stabilities of the electronic structures of the semiquinones compared to the quinone and quinol.

Similarly to the *p*-quinones, the Gibbs energies of reaction were corrected by adding 4.15 kJ/mol to each reduction step for 1,2-HBQ and 6.75 kJ/mol for the steps involving 1,2-HNQ and 9,10-HPQ. The corrections correspond to half the correction used for the 2 e^-, 2 H^+ reduction of the *o*-quinone to the *o*-quinol. Both calculated and corrected values for $\Delta_rG°$ are shown in Table 10.

Gibbs energies of reaction in water ($\Delta_rG°_{aq}$), calculated using the previously described methodology, are shown in Table 11. The calculated values were used for obtaining the differences in Gibbs energies of solvation ($\Delta_rG°_{solv}$) and standard potentials ($E°$(calc)). Values of ($E°$(corr)) for the Q/QH$^\bullet$ and QH$^\bullet$/QH_2 couples were calculated based on the corrections to $\Delta_rG°$ in Table 11, i.e., assuming that the energy underestimate is equally distributed over the two redox couples. The Gibbs energies of solvation ($\Delta G°_{solv}$) for each of the semiquinones are shown in Table 10. The main contribution to the stabilization by water (13−14 kJ/mol) corresponds to the QH$^\bullet$/QH_2 redox couple. This is different from the *p*-semiquinones but a consequence of the hydrogen bond between the C−OH and C═O groups, which limits the solvation energy as discussed for the quinols. Comparisons of the calculated and corrected potentials for the couples involved in the reduction of the *o*-quinones are shown in Figure 6.

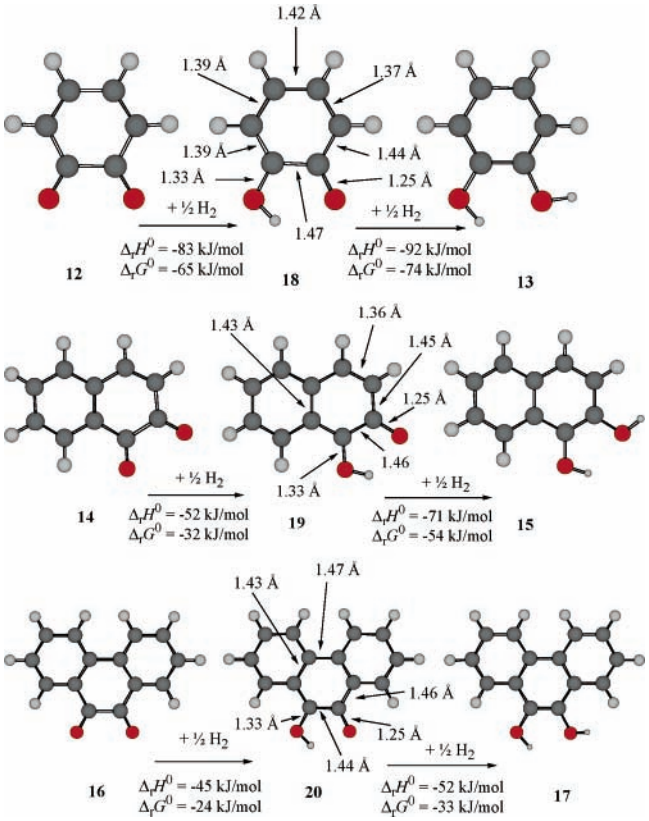

Figure 5. Optimized structures of neutral *o*-semiquinones (monohydroquinones), shown together with the corresponding quinones and quinols. The values of $\Delta_rH°$ and $\Delta_rG°$ for the two reduction steps and for some selected bond lengths are shown. Results obtained using B3LYP/6-311+G(d,p). 1,2-semibenzoquinone (**18**), 1,2-seminaphthoquinone (**19**), and 9,10-semiphenanthrenequinone (**20**).

All the calculated and corrected potentials for the Q/QH$^\bullet$ couple in Table 12 are less positive than those determined for the QH$^\bullet$/QH_2 couple. However, the two couples differ much less for the reduction of 1,2-BQ and 9,10-PQ, than for the other four quinones. This effect is observed for the difference in the $E°$ values between the two couples, which corresponds to the two times ($n_e = 2$) the potentials for the disproportionation reactions (1,2-BQ, 0.13 V; 1,2-NQ, 0.21 V; 9,10-PQ, 0.10 V). This trend is due to that the Gibbs energies for the disproportionation reactions of 1,2-HBQ and 9,10-HPQ in water are approximately half of those found for 1,2-HNQ and the three *p*-semiquinones.

3.3. Calculation of Potential Shifts. It is possible to avoid the use of additive corrections by calculating the shift in standard potentials when the *p*- and *o*-forms of a particular quinone are considered. This technique follows the same principle as the isodesmic reactions that were employed by Reynolds,[18−20] Rzepa et al.,[23] and Namazian et al.[24−30] Thus, it relies on the cancellation of errors when computing relative reaction energies for similar molecules. Three such isodesmic reactions are

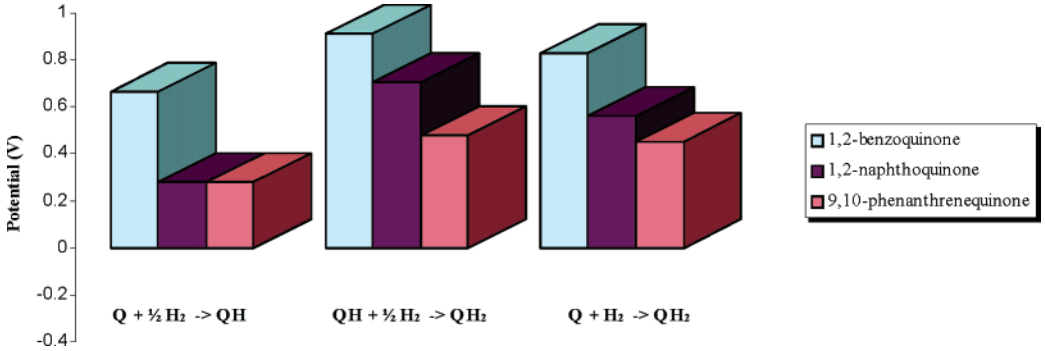

Figure 6. Calculated and corrected values ($E°$(corr)) for the reduction reactions Q + $^1/_2H_2$ → QH, QH + $^1/_2H_2$ → QH_2, and Q + H_2 → QH_2 for the three *o*-quinones.

TABLE 14: Calculated and Experimental Shifts (V) between the Standard Potentials of *p*- and *o*-Quinones[a]

$E°$(calc)[*p*-Q(aq) + H_2(g) → *p*-H_2Q(aq)] − $E°$(calc)[*o*-Q(aq) + H_2(g) → *o*-H_2Q(aq)]	$\Delta E°$(calc)/V	$\Delta E°$(exp)/V
$E°$(calc)[1,4-BQ(aq) + H_2(g) → *trans*-1,4-H_2BQ(aq)] − $E°$(calc)[1,2-BQ(aq) + H_2(g) →1,2-H_2BQ(aq)]	−0.138	−0.132 ± 0.016
$E°$(calc)[1,4-NQ(aq) + H_2(g) → *cis*-1,4-H_2NQ(aq)] − $E°$(calc)[1,2-NQ(aq) + H_2(g) → 1,2-H_2NQ(aq)]	−0.094	−0.077 ± 0.002
$E°$(calc)[9,10-AQ(aq) + H_2(g) → *trans*-9,10-H_2AQ(aq)] − $E°$(calc)[9,10-PQ(aq) + H_2(g) → 9,10-H_2PQ(aq)]	−0.374	−0.352 ± 0.03
$E°$(calc)[*p*-Q(aq) + $^1/_2H_2$(g) → *p*-HQ(aq)] − $E°$(calc)[*o*-Q(aq) + $^1/_2H_2$(g) → *o*-HQ(aq)]	$\Delta E°$(calc)/V	
$E°$(calc)[1,4-BQ(aq) + $^1/_2H_2$(g) → 1,4-HBQ(aq)] − $E°$(calc)[1,2-BQ(g) + $^1/_2H_2$(g) → 1,2-HBQ(g)]	−0.251	
$E°$(calc)[1,4-NQ(aq) + $^1/_2H_2$(g) → 1,4-HNQ(aq)] − $E°$(calc)[1,2-NQ(aq) + $^1/_2H_2$(g) → 1,2-HNQ(aq)]	−0.137	
$E°$(calc)[9,10-AQ(aq) + $^1/_2H_2$(g) → 9,10-HAQ(aq)] − $E°$(calc)[9,10-PQ(aq) + $^1/_2H_2$(g) → 9,10-HPQ(aq)]	−0.495	
$E°$(calc)[*p*-HQ(aq) + $^1/_2H_2$(g) → *p*-H_2Q(aq)] -$E°$(calc)[*o*-HQ(aq) + $^1/_2H_2$(g) → *o*-H_2Q(aq)]	$\Delta E°$(calc)/V	
$E°$(calc)[1,4-HBQ(aq) + $^1/_2H_2$(g) → *trans*-1,4-H_2BQ(aq)] − $E°$(calc)[1,2-HBQ(aq) + $^1/_2H_2$(g) → 1,2-H_2BQ(aq)]	−0.024	
$E°$(calc)[1,4-HNQ(aq) + $^1/_2H_2$(g) → *cis*-1,4-H_2NQ(aq)] − $E°$(calc)[1,2-HNQ(aq) + $^1/_2H_2$(g) → 1,2-H_2NQ(aq)]	−0.051	
$E°$(calc)[9,10-HAQ(aq) + $^1/_2H_2$(g) → *trans*-9,10 H_2AQ(aq)] − $E°$(calc)[9,10-HPQ(aq) + $^1/_2H_2$(g) → 9,10-H_2PQ(aq)]	−0.252	

[a] Notes: Values were calculated using data from Tables 3, 6, 9 and 12.

considered in Table 14:

$$p\text{-Q} + o\text{-QH}_2 \rightarrow p\text{-QH}_2 + o\text{-Q} \quad \text{(III)}$$

$$p\text{-Q} + o\text{-QH} \rightarrow p\text{-QH} + o\text{-Q} \quad \text{(IV)}$$

$$p\text{-QH} + o\text{-QH}_2 \rightarrow p\text{-QH}_2 + o\text{-QH} \quad \text{(V)}$$

In the case of reaction III, the calculation of the shifts is based on $E°$(calc) and the available $E°$(exp) values In contrast, no experimental potentials are available for the neutral semiquinones and hence no experimental shifts can be associated with IV and V. It is gratifying to note that the calculated shifts for the reactions involving 1,2-BQ and 1,4-BQ as well as 9,10-AQ and 9,10-PQ are within the error bars of the experimental shifts (see Table 14). The calculated shift in the comparison involving 1,2-NQ and 1,4-NQ is 15 mV larger than the experimental shift. This deviation corresponds to a discrepancy in the Gibbs energy of reaction, which is less than 3 kJ/mol. This could be due to incomplete cancellation of errors in the calculated energies (i.e., that the reductions of 1,2-NQ and 1,4-NQ are not fully comparable), but it could also reflect experimental uncertainties. From the quantum chemical point of view, the error is smaller than the average error in the B3LYP method and could therefore just reflect the inexactness of the exchange-correlation functional.

4. Conclusions

The thermodynamic functions for the reduction of quinones have been calculated using quantum chemical methods. Two effects were found to be particularly important:

(1) The replacement of C═C double bonds with aromatic bonds in the sequence benzo-, naphtho-, and anthraquinone (phenanthrenequinone) for both *p*- and *o*-quinones lowers the enthalpies and Gibbs energies of reduction.

(2) The reduction energies and enthalpies of the *o*-quinones were significantly more negative compared with those of the *p*-quinones. This is due to (a) elongation of the OC−CO single bonds caused by the repulsion between the C═O units and (b) interference between the aromatic side rings in 9,10-PQ. No such effects were observed for the *p*-quinones.

Furthermore, *o*- and *p*-quinones were found to display differences in the reaction energies toward formation of the neutral semiquinones. While it was concluded that the QH radical is an unstable intermediate in the reduction of *p*-quinones, its stability was significantly enhanced for the *o*-quinones. This was concluded from the very different Gibbs energies in the gas-phase for the disproportionation reactions, in which two QH radicals form one quinone and one quinol molecule. This difference is a further manifestation of the observation (2a) above. The effect of solvation was found to make the two quinone types more similar with respect to disproportionation. Indeed, 1,2-HBQ and 9,10-HPQ were found less prone to disproportionate than were the *p*-semiquinones and 1,2-HNQ.

The convergence of reduction enthalpies and energies with respect to the size of the basis set was investigated. Although the effect are smaller for B3LYP than for MP2 and CCSD(T), quite large basis sets are required for all methods. The most accurate B3LYP results were obtained using the 6-311+G(2df,-2pd) or 6-311+G(3df,3pd) basis sets. For these, the errors (<7 kJ/mol) in the converged reaction energies are below the 9.3 kJ/mol[52] average error of the B3LYP method. Most of the basis set effects can be compensated for by adding corrections to the results produced with the 6-311+G(d,p) basis set. The effect of using the incomplete 6-311+G(d,p) basis set was to underestimate the energetics of the 2 e^-, 2 H^+ reduction by

approximately 6 kJ/mol. In addition, the estimated errors in the exchange-correlation functional for the full reduction reactions were determined to 2.3 kJ/mol for the BQs and 7.5 kJ/mol for the NQs, AQ and PQ.

Standard potentials were calculated including systematic corrections for the overall reduction reactions, as well as for the formation of neutral semiquinones. For the $Q + H_2 \rightarrow QH_2$ reactions, all the calculated potentials ($E°$(corr)) were in good agreement with experimental values. Therefore, the $\Delta_r G°$(corr) and $\Delta_r G°_{aq}$(corr) values are probably the best theoretical estimates for the Gibbs energies of reduction for the reactions presented in this work. Similarly, the corrected potentials are probably the best estimates available for the stepwise reduction of both *p*-quinones and *o*-quinones at pH = 0. Isodesmic reactions were used to calculate the shifts in standard potentials between *p*-quinones and the corresponding *o*-quinones. Potential shifts were computed from the $E°$(calc) values and are thus not dependent on corrections to the B3LYP results. Experimental potentials were used to calculate potential shifts for the *p*-Q + *o*-$QH_2 \rightarrow$ *p*-QH_2 + *o*-Q reaction. The close agreement between experimental and calculated shifts for this reaction validates the computational procedure, and thus the predictions of the standard potential shifts for the stepwise reduction reactions.

Acknowledgment. This work was supported by the European Union "Clean Technologies for Peroxide Generation" (CLETEPEG, Contract No. G5RD-CT-2001-00463) and "Nanostructures for Energy and Chemicals Production" (NENA, Contract No NMP3-CT-2004-505906) projects. J.R.T.J.W. has also been supported by the foundation Blanceflor Boncompagni-Ludovisi, née Bildt. The National Supercomputing Center (NSC) in Linköping, Sweden, is gratefully acknowledged for a generous allocation of computer time through the Swedish national system for allocation of high-level computational resources (SNAC).

Supporting Information Available: Table S1, calculated energies for the gas phase reduction of quinones to yield the corresponding quinols, using different methods and basis sets, and text dicussing the table. This material is available free of charge via the Internet at http://pubs.acs.org.

References and Notes

(1) Mathews, C. K.; van Holde, K. E.; Ahern, K. G. *Biochemistry*, 3rd ed.; Benjamin Cummings: San Francisco, CA, 2000.

(2) Mitchell, P.; Moyle, J. *Eur. J. Biochem.* **1969**, *9*, 149.

(3) Thomson, R. H. *Naturally occurring quinones I−IV*; Butterworth Scientific Publ.: London, 1957; Academic Press: London, 1971; Chapman & Hall: London, 1987; Blackie Academic & Professional: London, 1997.

(4) Papageorgiou, V. P.; Assimopoulou, A. N.; Couladouros, E. A.; Hepworth, D.; Nicolaou, K. C. *Angew. Chem., Int. Ed. Engl.* **1999**, *38*, 270.

(5) (a) Link, T. A. *FEBS Lett.* **1997**, *412*, 257. (b) Sharp, R. E.; Palmitessa, A.; Huang, L.-S.; Kuras, R.; Zhang, Z.; Berry, E. A. *Biochemistry* **1999**, *38*, 15791. (c) Brandt, U. *J. Bioenerg. Biomembr.* **1999**, *31*, 243.

(6) Greenwood, N. N.; Earnshaw, A. *Chemistry of the Elements*, 2nd ed.; Butterworth-Heinemann: Oxford, U.K., 1997; Chapter 14.

(7) Tammeveski, K.; Kontturi, K.; Nichols, R. J.; Potter, R. J.; Schiffrin, D. J. *J. Electroanal. Chem.* **2001**, *515*, 101.

(8) Sarapuu, A.; Vaik, K.; Schiffrin, D. J.; Tammeveski, K. *J. Electroanal. Chem.* **2003**, *541*, 23.

(9) Vaik, K.; Schiffrin, D. J.; Tammeveski, K. *Electrochem. Commun.* **2004**, *6*, 1.

(10) Mirkhalaf, F.; Tammeveski, K.; Schiffrin, D. J. *Phys. Chem. Chem. Phys.* **2004**, *6*, 1321.

(11) Vaik, K.; Sarapuu, A.; Tammeveski, K.; Mirkhalaf, F.; Schiffrin *J. Electroanal. Chem.* **2004**, *564*, 159−166.

(12) Boesch, S. E.; Wheeler, R. A. *J. Phys. Chem. A* **1997**, *101*, 5799.

(13) Balakrishnan, G.; Mohandas, P.; Umapathy, S. *Spectrochim. Acta, Part A* **1997**, *53*, 1553.

(14) Burie, J.-R.; Boullais, C.; Nonella, M.; Mioskowski, C.; Nabedryk, E.; Breton, J. *J. Phys. Chem. B* **1997**, *101*, 6607.

(15) Grafton, A. K.; Boesch, S. E.; Wheeler, R. A. *J. Mol. Struct. (THEOCHEM)* **1997**, *392*, 1.

(16) Razeghifard, M. R.; Kim, S.; Patzlaff, J. S.; Hutchinson, R. S.; Krick, T.; Ayala, I.; Steenhuis, J. J.; Boesch, S. E.; Wheeler, R. A.; Barry, B. A. *J. Phys. Chem. B* **1999**, *103*, 9790.

(17) Kaupp, M.; Remenyi, C.; Vaara, J.; Malkina, O. L.; Malkin, V. G. *J. Am. Chem. Soc.* **2002**, *124*, 2709.

(18) Reynolds, C. A.; King, P. M.; Richards, W. G. *J. Chem. Soc., Chem. Commun.* **1988**, 1434.

(19) Reynolds, C. A.; King, P. M.; Richards, W. G. *Nature (London)* **1988**, *334*, 80.

(20) Reynolds, C. A. *J. Am. Chem. Soc.* **1990**, *112*, 7545.

(21) Wheeler, R. A. *J. Am. Chem. Soc.* **1994**, *116*, 11048.

(22) Raymond, K. S.; Grafton, A. K.; Wheeler, R. A. *J. Phys. Chem. B* **1997**, *101*, 623.

(23) Rzepa, H. S.; Suñer, G. A. *J. Chem. Soc., Chem. Commun.* **1993**, 1743.

(24) Jalali-Heravi, M.; Namazian, M.; Peacock, T. E. *J. Electroanal. Chem.* **1995**, *385*, 1.

(25) Jalali-Heravi, M.; Namazian, M. *J. Electroanal. Chem.* **1997**, *425*, 139.

(26) Namazian, M.; Almodarresieh, H. A. *J. Mol. Struct. (THEOCHEM)* **2004**, *686*, 97.

(27) Namazian, M.; Almodarresieh, H. A.; Noorbala, M. R.; Zare, H. R. *Chem. Phys. Lett.* **2004**, *396*, 424.

(28) Namazian, M.; Norouzi, P. *J. Electroanal. Chem.* **2004**, *573*, 49.

(29) Namazian, M.; Norouzi, P.; Ranjbar, R. *J. Mol. Struct. (THEOCHEM)* **2003**, *625*, 235.

(30) Namazian, M. *J. Mol. Struct. (THEOCHEM)* **2003**, *664−665*, 273.

(31) Rosso, K. M.; Smith, D. M. A.; Wang, Z.; Ainsworth, C. C.; Fredrickson, J. K. *J. Phys. Chem. A* **2004**, *108*, 3292.

(32) Eriksson, L. A.; Himo, F.; Siegbahn, P. E. M.; Babcock, G. T. *J. Phys. Chem. A* **1997**, *101*, 9496.

(33) Manojkumar, T. K.; Choi, H. S.; Tarakeshwar, P.; Kim, K. S. *J. Chem. Phys.* **2003**, *118*, 8681.

(34) Conant, J. B.; Fieser, L. F. *J. Am. Chem. Soc.* **1924**, *46*, 1858.

(35) Proudfoot, G. M.; Ritchie, I. M. *Aust. J. Chem.* **1983**, *36*, 885.

(36) Hale, J. M, Parsons, R. *Trans. Faraday Soc.* **1963**, *59*, 1429.

(37) Kano, K.; Uno, B. *Anal. Chem.* **1993**, *65*, 1088.

(38) Driebergen, R. J.; den Hartigh, J.; Holthuiss, J. J. M.; Hulshoff, A.; van Oort, W. J.; Postma Kelder, S. J.; Verboom, W.; Reindhoudt, D. N.; Bos, M.; van der Linden, W. E. *Anal. Chim. Acta* **1990**, *133*, 251.

(39) Bailey, S. I.; Ritchie, I. M. *Electrochim. Acta* **1985**, *30*, 3.

(40) LaMer, K. V.; Baker, L. E. *J. Am. Chem. Soc.* **1922**, *44*, 1954.

(41) Schreurs, J.; van den Berg, J.; Wonders, A. Barendrecht, E. *Pays-Bas.* **1984**, *103*, 251.

(42) Hu, I.-F.; Karweik, D. H.; Kuwana, T. *J. Electroanal. Chem.* **1985**, *188*, 59.

(43) Clark, M. W. *Oxidation Reduction Potentials of Organic Systems*, Baillière, Tindall & Cox Ltd.: London, 1960.

(44) Binder, H.; Köhling, A.; Sandstede, G. *Ber. Bunsen-Ges. Phys. Chem.* **1976**, *80*, 66.

(45) DuVall, S. H.; McCreery, R. L. *J. Am. Chem. Soc.* **2000**, *122*, 6759.

(46) Tammeveski, K.; Kontturi, K.; Schiffrin, D. J. Unpublished results.

(47) Sarapuu, A.; Helstein, K.; Schiffrin, D. J.; Tammeveski, K. *Electrochem. Solid State Lett.* **2005**, *8*, E30.

(48) Brown, A. P.; Koval, C.; Anson, F. C. *J. Electroanal. Chem.* **1976**, *72*, 379.

(49) Brown, A. P.; Anson, F. C. *Anal. Chem.* **1977**, *49*, 1589.

(50) Cheng, H. Y.; Falat, L.; Li, R.-L. *Anal. Chem.* **1982**, *54*, 1384.

(51) Fieser, L. F.; Ames, M. A. *J. Am. Chem. Soc.* **1927**, *49*, 2604.

(52) Becke, A. D. *J. Chem. Phys.* **1993**, *98*, 5648.

(53) Johnson, J. R. T.; Panas, I. *Inorg. Chem.* **2000**, *39*, 3181. Johnson, J. R. T.; Panas, I. *Inorg. Chem.* **2000**, *39*, 3192. Johnson, J. R. T.; Panas, I. *Chem. Phys. Lett.* **2001**, *348*, 433. Johnson, J. R. T.; Panas, I. *Phys. Chem. Chem. Phys.* **2001**, *3*, 5482. Johnson, J. R. T.; Panas, I. *Chem. Phys.* **2002**, *276*, 45. Johnson, J. R. T.; Panas, I. *J. Phys. Chem. A* **2002**, *106*, 184.

(54) (a) *Gaussian 98, Revision A.11.4* Frisch, M. J.; et al. Gaussian, Inc.: Pittsburgh, PA, 2002. (b) *Gaussian 03, Revision C.02*; Frisch, M. J.; et al. Gaussian, Inc.: Wallingford CT, 2004.

(55) Ochterski, J. W. *Thermochemistry in Gaussian*, available at http://www.gaussian.com/g_whitepap/thermo.htm.

(56) Krishnan, R.; Binkley, J. S.; Seeger, R.; Pople, J. A. *J. Chem. Phys.* **1980**, *72*, 650.

(57) Clark, T.; Chandrasekhar, J.; Spitznagel, G. W.; v. R. Schleyer, P. *J. Comput. Chem.* **1983**, *4*, 294.

(58) Cossi, M.; Scalmani, G.; Rega, N.; Barone, V. *J. Chem. Phys.* **2002**, *117*, 43.

(59) Anderson, A. B.; Albu, T. V. *J. Am. Chem. Soc.* **1999**, *121*, 11855.
(60) Narayanasamy, J.; Anderson, A. B. *J. Phys. Chem. B* **2003**, *107*, 6898.
(61) Johnsson Wass, J. R. T. Unpublished results. B3LYP and 6-311+G-(d,p) were used in these calculations.
(62) Tissandier, M. D.; Cowen, K. A.; Feng, W. Y.; Gundlach, E.; Cohen, M. H.; Earhart, A. D.; Coe, J. V.; Tuttle, T. R., Jr. *J. Phys. Chem. A* **1998**, *102*, 7787.
(63) Lide, David R., Ed. *CRC Handbook of Chemistry and Physics, Internet Version 2005*; CRC Press: Boca Raton, FL, 2005; http://www.hbcpnetbase.com.
(64) Ribiero da Silva, M. A. V.; Ribiero da Silva, M. D. M. C. *J. Chem. Thermodyn.* **1988**, *20*, 969.
(65) Ribiero da Silva, M. A. V.; Ribiero da Silva, M. D. M.; Teixeira, J. A. S.; Bruce, J. M.; Guyan, P. M.; Pilcher, G. C. *J. Chem. Thermodyn.* **1989**, *21*, 265.